Optimal emergency response to maritime oil spills under dynamic demand and supply of resources

Abstract: During an emergency response to a major oil spill accident, the features of the motion of the oil film affect the response decisions. A highly dynamic optimal solution is needed to tackle the continuous changes in the demand for emergency resources and transportation networks for logistics deliveries that must occur. To effectively balance the responsiveness and response cost in the emergency logistics operation, this paper proposes a dynamic multi-objective location-routing model to address new challenges such as the time-varying demands of contaminated areas, the dynamic state of the associated transportation networks and the interrelationship between the changes in spilled oil films and emergency operations. Since the problem is NP-hard, to efficiently obtain Pareto solutions, a novel implementation of a heuristic framework based on particle swarm optimization is developed to conduct numerical experiments. Additionally, to handle the multi-objective model, an alternative solution based on the cost performance method is adopted to help decision makers select the ideal options for Pareto solutions. A case study of a major oil spill accident that occurred in the Bohai Bay is conducted to demonstrate the application of the proposed model and approaches and the real-world implications.

Keywords: OR in disaster relief; Maritime emergency logistics; Oil spill; Location-routing problem; Multi-objective optimization

1 Introduction

Offshore oil exploration and production facilities and tanker vessels are the major sources of accidental oil spills in the marine environment (Payam et al., 2019). With the fast development of offshore oil exploration and the increase in the amount of crude oil shipped by sea, the risk of major maritime oil spill accidents is increasing year by year. Although the statistics indicate a declining number of oil spills due to the technical advancement and more stringent regulations, major spills still frequently occur, which may lead to serious economic losses and immeasurable damage to the marine ecological environment (Ye et al., 2019).

Here are some recent examples. The Deepwater Horizon Oil Spill that occurred in the Gulf of Mexico in 2010 released with a total cleanup cost of over $14 billion. After the major oil spill occurred, the U.S. National Commission on the Deepwater Horizon Oil Spill and Offshore Drilling, relying on the Oil Pollution Act, immediately activated the national, regional and local emergency command systems and promptly took measures to stop, control and recycle the spilled oil. In response to the emergency, over 39,000 personnel, 5000 vessels and 110 aircraft were dispatched, over 700 km of booms were deployed, 275 controlled burns were carried out, approximately 27 million gallons of oil-water mixture were recycled by skimmers, and more than 1.5 million gallons of dispersants were used. However, improper emergency resource scheduling decisions can not only affect the operation efficiency of oil recovery but also cause waste in terms of manpower and budgets (U.S. National Commission on the Deepwater Horizon Oil Spill and Offshore Drilling, 2011). More recently, the Panamanian-flagged tanker Sanchi, which was carrying 110,000 tons of condensate oil collided with the Hong Kong-flagged cargo ship CF Crystal at approximately 160 nautical miles east of the Yangtze Estuary on January 6, 2018, which resulted in the Sanchi catching fire and eventually sinking, and a large amount of cargo oil and fuel oil spilled into the water. As a result, the total cleanup area spanned 225.8 square nautical miles. After the accident, the State Council attached great importance to it. Under the command of the Ministry of Transport in China, the transportation emergency system mobilized a great number of vessels, professionals and emergency resources from different regional/provincial administrations such as the East China Sea Rescue Bureau and the Shanghai Salvage Bureau to overcome the various difficulties related to searching for people in distress and cleaning up the spilled oil.

These events have created a strong shockwave globally in the industry, the government, as well as the research community. Consequently, tremendous amount of research efforts have been made in the areas of contingency policy, risk and impact assessment, and response technique development (Daley et al., 2016; Xiong et al., 2020; Barron et al., 2012). In

comparison, there are limited studies which are devoted to the development and implementation of process optimization and decision making in maritime emergency logistics.

Emergency logistics consists of several operations such as pre-arranged planning, mitigation, warehousing and transportation (Torabi et al., 2018). In general, these operations can be classified in two aspects, including pre-disaster phase (e.g., the pre-positioning of critical emergency resources) and post-disaster phase (e.g., the emergency resource scheduling) (Moreno et al., 2018). At present, great progress has been made in the research on pre-disaster emergency logistics at sea. Considering the influence of maritime natural conditions, Ai et al. (2016) propose an optimization model to address the problem of location, allocation and configuration in the pre-disaster phase. Sarhadi et al. (2020) present a robust optimization approach to the problem of designing emergency response networks for marine oil spills given uncertainty in the location, size and type of the spill. Zhang et al. (2017b) propose a maritime emergency resource allocation model with a robust approach to deal with the uncertainty of location, type and severity of oil spills. However, the research on post-disaster maritime emergency logistics is still in preliminary exploration. The reviewed literature reveals that the relevant studies hold strong assumptions, which neglect the dynamic motion of oil films and are inconsistent with the real situations. Although these studies have tried to optimize the maritime emergency resource scheduling, they generally have the issues of improper data modeling and assumptions, which can be a reason why field-based decision makers are reluctant to use the analytic models. Compared to the emergency logistics studies on maritime emergency logistics, land-based emergency logistics problems have attracted much more attention from the research community and been extensively studied in recent decades (Sheu, 2007; Yang et al., 2019). The context of operations after sudden-onset land-based disasters can be dynamic and sophisticated. Emergency resources can change over the course of the response efforts depending on conditions, such as weather and secondary disasters. Similarly, the transportation infrastructure status may change rapidly. Therefore, a great number of studies on land-based emergency logistics attempt to address dynamic issues in the emergency response efforts and propose a series of theoretical methods to reflect the uncertain factors (Loree et al., 2018; Maharjan et al., 2020; Cao et al., 2018; Zhang et al., 2019). Although the relevant research results show that these methods can effectively deal with the problem of land-based emergency resource scheduling, they are not effective in the response efforts to oil spills as we will explain specifically in Section 2. Therefore, how to avail of advanced modeling approaches to improve the efficiency of response operations with consideration of dynamic changes of oil spills has been recognized as a vital and urgent task in the field.

A successful sudden-onset disaster response should meet the needs of effectiveness in the shortest amount of time (responsiveness) with the least amount of resources (cost efficiency) (Hu et al., 2016; Kunz et al., 2017; Baharmand, 2019). Improving responsiveness and cost efficiency is one of the main challenges profoundly influenced by emergency resource scheduling directly and indirectly. To mitigate the damage of oil spills on the ecological environment and the threat to potential contaminated areas, the relevant departments are required to coordinate to optimally use the available manpower and resources during emergency response efforts. A scientific and efficient emergency resource scheduling methodology can tremendously reduce the negative impacts caused by oil spills and maximize the responsiveness based on the emergency resources required. What's more, very limited studies exist in the literature addressing the problem of emergency resource scheduling for the response efforts to oil spills and it is still an open research field. In this regard, we have also conducted some interviews with several officials from the Maritime Safety Administration of China who have participated in the response efforts to the Conocophillips oil spill in 2011 and the Sanchi oil spill in 2018. They approve that due to the lack of theoretical decision support, the scheduling of oil spill emergency materials usually relies on subjective experience, and even sometimes there is a chaotic situation in which all parties take their own actions. Hence, there is an urgent need to improve responsiveness the emergency resource scheduling in the response efforts to oil spills. Keeping this in mind and referring to the current literature motivate us to develop a novel emergency resource scheduling methodology for maritime oil spill emergency response efforts in which the dynamic demand (of the emergency resources) and uncertain

transport networks (connecting multiple supply points) are well incorporated to balance responsiveness and the total response cost.

The remainder of this paper is organized as follows. In Section 2, a literature review of emergency logistics problems is conducted to reveal the research gap in the field. Section 3 describes the problem definition and model conceptualization framework. In Section 4, the model for the optimal scheduling of emergency resources in response to a large-scale maritime oil spill is developed. In Section 5 we propose an improved multi-objective particle swarm optimization (IMPSO) algorithm and adopt an alternative quantitative method to select the optimal option from the set of Pareto non-dominated solutions. The newly developed model and algorithm are applied in a case study and a series of sensitivity analyses are undertaken to test the performance of the proposed model and approaches in Section 6. Finally the conclusions are drawn in Section 7.

2 Literature review

The emergency logistics features in disaster response situations are critical for decision making (Wang et al., 2014a). In terms of the emergency response to oil spills, the uncertainty caused by the oil film dynamic motion is the most prominent feature. Emergency logistics problems have been extensively studied in recent decades. Especially in recent years, numerous studies in the literature of land-based emergency logistics tend to delve into the dynamic issues in the emergency response, which provide many valuable references for our work. So the first stream of the reviewed literature concerns modeling approaches for dynamic issues in land-based emergency logistics. In addition, oil spill emergency resource scheduling is essentially a maritime emergency logistics problem. Therefore, another stream focuses on the problems of scheduling emergency resources for chemical spills at sea.

Tackling the uncertainty in an emergency response situation is vital for the success of emergency logistics operations when large-scale disasters occur (Sheu, 2010). To address the issues of dynamic emergency demands and uncertainty in the state of the transportation networks during the crucial rescue period of a large-scale land-based disaster, the following three methods have been widely used in the literature, 1) the time period planning horizon (e.g., Abdolhamid et al., 2020; Song et al, 2017; Loree et al., 2018; Maharjan et al., 2020), 2) the rolling planning horizon (e.g., Daniel et al., 2020; Lu et al, 2016; Huang et al., 2015; Cao et al., 2018) and 3) the scenario planning approach (e.g., Gökalp et al., 2020; Zhang et al., 2019; Ahmadi et al., 2015; Alem et al., 2016; Rezaei-Malek et al., 2016). The time period planning horizon divides the response phase into several fixed time periods so that a complicated dynamic problem is transformed into a relatively static problem that is easier to address (Hoyos et al., 2015). In the rolling planning horizon, multiple planning horizons are considered and the parameters of the model can be updated at the beginning of each horizon. According to Huang et al. (2015), this approach effectively addresses the uncertainties in disaster response situations because decisions can be revised at several key time points based on the available real-time information. Additionally, in the scenario planning approach, the uncertainty is addressed by probabilistic scenarios representing dynamic demands and the state of the transportation networks (Zhang et al., 2019). The scenarios and their associated probabilities can be devised on the basis of the historical records and know geological faults.

Despite substantial economic losses and large-scale ecological environmental damage caused by major oil spills, the existing literature has primarily focused on land-based disasters (Huang et al., 2020). Surprisingly, there are just few studies that address emergency logistics problems in the response efforts to chemical spills at sea. Due to the specifics of maritime peril and rescue at sea, Wang et al. (2014b) present a two-phase collaborative scheduling model for rescue resources around an object in distress from the sea and inland. However, this work is based on the hypothesis that once the emergency force reaches the object, drift will no longer occur, which does not substantially address the problem of emergency resource scheduling for the objects in distress with dynamic motion. Huang et al. (2020) propose a multi-objective optimization model of scheduling emergency resources for oil spills based on the similar hypothesis to that of Wang et al. (2014b). There is no doubt that their work also ignores the dynamic motion of the oil films. Liu et al. (2018) propose an emergency resource allocation

model based on a time-varying supply-demand constraint, using linear functions to represent the changes in the supply amount available at the multiple potential supportive centers and the demand amount of the single demand point. Nevertheless, this model is not qualified to incorporate the interrelationship between emergency resource allocation and changes in the chemical spill. Hao et al. (2020) make use of a triangular fuzzy method to reflect the uncertainty in the demand for emergency resources and in the scheduling time during the response to oil spills, in which the dynamic issues are transformed into a static fuzzy problem by overlooking the dynamic motion of the oil films. Garrett et al. (2017) develop a mixed-integer linear programming model based on the time period planning horizon to address the dynamic resource allocation challenges which are faced by an Arctic oil spill response network. They make use of the approach (i.e., the time period planning horizon) proposed for land-based emergency logistics to solve the problem of scheduling emergency resources for oil spills, which undoubtedly converts the continuous dynamic motion of oil films into the periodic dynamic motion, and is obviously inconsistent with the reality.

To facilitate the literature analysis, we present the reviewed studies in Table 1. It classifies the reviewed studies according to fourteen criteria classified in three classes which are model features, data modeling and decisions. Nevertheless, there are several defects to the proposed models and approaches of the reviewed literature when they are applied to the oil spill emergency response. These defects are summarized as follows.

At first, the approaches (in Columns 7-9 of Table 1) applicable to land-based emergency response situations are not necessarily applicable within the context of the dynamic emergency response required for oil spills at sea. Most of the existing models are mainly developed to cope with the emergency response to land-based disasters. Even under such conditions, the emergency resource scheduling strategy encompasses rather difficult tasks to accomplish. These challenging situations may become even more complicated when the decision making relies on the uncertainty of the changing marine environment. As far as the uncertainty is concerned, the scenario planning approach (i.e., Scenario planning) largely targets long-term decision making and strategic planning (Charles et al. 2016). Although this approach is obviously superior to the static approach (i.e., Static) that often ignores the uncertainty presented in practice, it is not very efficient when contending with real-world problems (Najafi et al., 2013). While the common assumption of the other existing emergency logistics models (e.g., the time period planning horizon (i.e., Time planning) and the rolling planning horizon (i.e., Rolling planning)) is that the demand for emergency resources and the state of transportation networks in the affected areas remain relatively stable at different time intervals (Hoyos et al., 2015; Huang et al., 2015). Only when the emergency response phase reaches key specific time points will the demand and transportation network state in the system change and be updated accordingly. In the emergency response efforts for maritime oil spills, such an assumption is absolutely not acceptable. The dynamic motion of the oil films are constantly changeable, which critically affect the decisions regarding the emergency response efforts to oil spills. Due to the action of surface tension, oil films at sea continuously diffuse, resulting in the continuous expansion of the contaminated areas. Since the consumption of emergency resources is usually positively correlated with the size of an oil film area, the demands in the response phase correspondingly increase with the diffusion of the oil films. Moreover, the oil films will drift by the forces of waves and currents, and therefore, the transportation networks of the emergency vessels have to be dynamically adjusted to coordinate the emergency resources from different supply points. The abovementioned dynamic processes are all continuous without pauses and do not fit the periodical changes modeled in the existing methods. In order to ensure the effectiveness of decisions on oil spill emergency resource scheduling, the dynamic motion of the oil films is absolutely not allowed to be ignored. Unfortunately, most of the existing studies on the scheduling of emergency resources for chemical spills usually ignore the dynamic motion of the oil films (Hao et al., 2020; Garrett et al., 2017) or avoid discussing the drift and diffusion of the oil films by setting assumptions (Wang et al., 2014b; Huang et al., 2020), so as to simplify the scheduling problem. The problems of rapid and continuous scenario updates can be solved via dynamic optimization models with time-varying features. However, very few studies have incorporated rapid scenario

updates in crisis decision making (Comes et al., 2015). Hence, it leaves us a research opportunity to creatively take into consideration dynamic issues caused by oil film diffusion and drift via the time-varying planning approach (i.e., Time-var. planning).

Second, few studies have taken into consideration the influence of emergency operations on the demand for emergency resources and the transportation networks. The reviewed studies, including both the studies of land-based emergency logistics and those of maritime emergency logistics, mainly focus on the impact of the uncertainty of the decision-making environment on emergency logistics distribution (e.g., Daniel et al., 2020; Loree et al., 2018; Hao et al., 2020; Garrett et al., 2017). As the oil films exhibit dynamic motion due to diffusion and drift, there is an interrelationship between the oil film changes and emergency resource scheduling. On one hand, there is no doubt that the changes in the oil film size and position affect the scheduling decisions, while on the other hand, the transportation and delivery of emergency resources impact the changes in the oil film motion. For example, if oil booms can be quickly transported to the demand point with a thick oil film and control the continuous diffusion of the oil film in time, the size of the polluted area at the demand point will be effectively decreased, thus reducing the demand for emergency resources. Such an interrelationship may be rare in the studies of land-based emergency logistics. In the problem of land-based emergency logistics, the emergency resources are usually food, water and medical supplies. Whether these resources arrive at the demand points in time is related to the intuitive feelings of people in the affected areas, but does not affect the demand amount. This also implies to some extent that the problem of maritime emergency logistics is more complicated than that of land-based emergency logistics. Nevertheless, none of the reviewed studies referring to chemical spills at sea has discussed the interrelationship as show in Column 6 of Table 1. Note that although Liu et al. (2018) adopt the similar approach to ours, the time-varying planning approach, to address the dynamic issues in the emergency response to oil spills, our work is significantly different from theirs. Their work is determined to use the linear functions with time to represent the time-varying demand and supply of emergency resources in the model, the relationship between demand and supply can be represented by a strict equation. It indicates that the exact demand amount of emergency resources at the demand point can be obtained by solving the strict equation, and is actually fixed and entirely determined by the linear functions. There is no room for flexible changes between supply and demand, which eliminates the basis for discussing the interrelationship between the external decision-making environment and the emergency operations. This interrelationship is one of the most prominent features of the oil spill emergency response. In order to ensure the efficiency of the scheduling decisions in practical, it must be taken seriously.

Third, most reviewed studies have proposed multi-objective optimization models to comprehensively consider responsiveness and cost efficiency in emergency response efforts (e.g., Maharjan et al., 2020; Abdolhamid et al., 2020; Huang et al., 2015; Alem et al., 2016). It is often the case to have the contradicting objectives in modeling multi-objective optimization problems. Therefore, it is difficult to find a unique optimal solution that can satisfy all the objectives. There are various approaches in the reviewed literature to solve multi-objective optimization problems and they are presented in Column 4 of Table 1 (i.e., Multi-obj. approach). To cope with such issues, some studies use a Pareto solution set as the result of the multi-objective optimization model. Obviously, this cannot provide an exact decision reference for decision making. Decision makers can only select an ideal logistics scheme from the Pareto solution set according to the subjective experience, which is hard to ensure the scientific nature and rationality of the final decision, especially when there exist numerous elements in the solution set. While the others use scalar methods (e.g., the weighed sum method, the epsilon constraint method) to transform a multi-objective model into a mono-objective one to avoid the tricky problem of selecting the optimal solution for the multi-objective problem (Zajac et al., 2020). However, there are still some drawbacks in these methods. The main idea of the weighed sum method is to assign a certain weight to each objective and convert the multi-objective problem into a mono-objective counterpart. The quality of the obtained optimal solution depends heavily on the assigned weight coefficient, and the setting of the weight often involves subjective bias, which triggers bias in the decision making for emergency logistics (Zhang et

al., 2019). In the epsilon constraint method, one of the objective functions is optimized by using the other objective functions as constraints and incorporating them into the constraint part of the model. In this way, it inevitably places too much emphasis on one of the optimization objectives at the expense of neglect of the others. Note that Zhang et al. (2019) develop a unique approach to deal with the multi-objective optimization problems, namely the fuzzy linear programming. This approach does not need to set weights in advance or convert some optimization objectives into the constraints, which reduces the subjectivity in selecting the ideal solution. However, there are still some shortcomings in the application of this approach in the field of emergency logistics research. The fuzzy linear programming has randomness when determining the ideal solution, and the selected solutions do not always attach most importance to responsiveness, which is inconsistent with the fundamental purpose of emergency logistics. An effective alternative method, which can avoid the subjectivity of the weight coefficient setting and ensure the robustness of the selected solutions, needs to be creatively proposed.

Motivated by these issues which are not addressed well, this paper presents a novel dynamic multi-objective location-routing model for oil spill emergency response. This model can help determine the emergency resource reserved bases (ERRBs) to constitute the emergency fleets to participate in the emergency response efforts, manage the routes of the emergency fleets and even dispatch vessels and allocation emergency resources to the emergency fleets, while taking into account the abovementioned important but unaddressed practical requirements, such as the time-varying demands of the contaminated areas, the dynamic state of the associated transportation networks and the interrelationship between the decision-making environment and emergency operations. To support the trade-offs between responsiveness and the response cost, this paper adopts an alternative solution based on the cost performance method to select the ideal solution for Pareto non-dominated solutions. Thus, the main contributions of our paper are as follows:

1 A novel time-varying planning approach is developed for the first time to represent the dynamic factors influencing the emergency response efforts to oil spills, which can better reflect the actual situations of the emergency response and improve the operation efficiency compared to the relatively static analysis in the conventional approaches.

2 The interrelationship between the external decision-making environment and emergency operations is taken into consideration in the decision-making process for the emergency response to oil spills in a pioneering way, which is one of the most prominent features of the oil spill emergency response but hardly mentioned by the reviewed studies.

3 A number of time-varying parameters in the proposed optimization model render it difficult to solve the model directly by conventional heuristic algorithms. Therefore, an improved algorithm with embedded iterative dynamic programming is developed to coordinate the interrelationship between the changes in spilled oil films and emergency operations, and corresponding improvement measures are proposed to improve the algorithm's computational efficiency as well.

4 An alternative solution based on the cost performance method is adopted to cope with the multi-objective models and help the decision makers select the ideal solution from Pareto non-dominated solutions.

Table 1
Overview of studies on emergency logistics related to this paper.

Reference	Model features					Data modeling					Decisions			
	Stream	Multi-objective	Multi-obj approach	Solution method	Int.	Time planning	Rolling planning	Scenario planning	Time-var. planning	Static	Location	Route planning	Fleet sizing	Resource allocation
Abdolhamid et al.（2020）	L	√	PS	NSGA-II		√					√			√
Cao et al. (2018)	L	√	WS	GA			√					√		√
Ahmadi et al. (2015)	L			EXC				√			√	√		√
Loree et al. (2018)	L			B-OA		√					√			√
Gökalp et al. (2020)	L			EXC				√			√			√
Maharjan et al. (2020)	L	√	EC	EXC		√					√			√
Daniel et al. (2020)	L			EXC			√					√	√	√
Zhang et al. (2019)	L	√	FLP	EXC				√						√
Lu et al. (2016)	L			EXC			√							√
Song et al. (2017)	L	√	PS	PSO		√								√
Rezaei-Malek et al. (2016)	L	√	PS	NSGA-II				√			√			√
Ghasemi et al. (2019)	L	√	PS	PSO				√			√			√
Huang et al. (2015)	L	√	WS	EXC			√							√
Alem et al. (2016)	L	√	WS	EXC				√				√	√	√
Wang et al. (2014a)	L	√	PS	NSGA-II						√	√	√		√
Rezaei et al. (2020)	L	√	PS+WS	NSGA-II						√	√			√
Wei et al. (2020)	L	√	PS	ACO						√	√			√
Garrett et al. (2017)	M			EXC		√					√			√
Huang et al. (2020)	M	√	PS	PSO						√			√	√
Wang et al. (2014b)	M			Greedy						√				√
Hao et al. (2020)	M	√	PS	NSGA-II						√				√
Liu et al. (2018)	M			Greedy					√					√
This paper	M	√	PS+CPM	PSO	√				√		√	√	√	√

L: land-based emergency logistics; M: maritime emergency logistics; PS: Pareto solutions; WS: the weighed sum method; EC: the epsilon constraint method; CPM: the cost performance method; FLP: the fuzzy linear programming; GA: the genetic algorithm; B-OA: the BONMIN outer approximation algorithm; NSGA-II: the non-dominating sorting genetic algorithm-II; Greedy: the greedy algorithm; PSO: the particle swarm optimization algorithm; ACO: the ant colony optimization algorithm; EXC: the exact approaches (e.g., CPLEX, GUROBI, LINGO and so on.); Int.: the interrelationship between the external decision-making environment and emergency operations.

3 Background to the problem

Here, we describe the practical problem as how to respond to a major oil spill accident by means of transporting and delivering emergency resources to the demand points at sea. In this decision-making process, we address the issue related to the dynamic motion of oil films, to which the existing methods fail to provide any effective solution.

3.1 Problem description

To simplify the maritime emergency resource transportation networks, we consider all the demand points and ERRBs as nodes, denoted by a set V. V includes two subsets, i.e., A and B ($V = A \bigcup B$). $A = \{1, 2, \cdots, n\}$ is the set of demand points, and $B = \{n+1, \cdots, n+m\}$ represents the set of ERRBs. The division of demand points is not entirely determined by the number and distribution of oil films. When a major maritime oil spill accident occurs, spilled oil diffuses rapidly and even spreads to other regions under the influence of waves and currents, thus causing a large polluted sea area (Xu et al., 2016). Due to the vastness of the contaminated area, the oil film conditions in diverse regions are significantly different, which necessitates different emergency resource requirements. Herein, the demand points need to be divided according to the characteristics of the oil films, which determines the types of emergency resources required. To simplify the analysis process, this paper only considers the contaminated regions in need of oil booms as the demand points and focuses on the scheduling problem of oil booms, which are the most widely used floating mechanical barriers to prevent the further spread of spilled oil and are generally applicable to thick oil films.

When constructing emergency resource scheduling schemes, decision makers should pay attention to the fact that the oil film has the characteristics of continuous diffusion and drift. First, since the consumption of emergency resources has a positive correlation with oil spill areas, when the oil film of a demand point spreads over time, the demand for emergency resources at the point will correspondingly increase. $d_i(t)$, which denotes that the emergency resource demand at point $i (i \in A)$, is not a fixed value but is a parameter changing with time t. In addition, the positions of the oil films constantly change due to drift motion, which will lead to a dynamic change in the transportation networks of emergency vessels. Similarly, the distance between nodes $i, j (i, j \in V)$, $dis_{ij}(t)$ is also a time-varying parameter. More importantly, in addition to how the dynamic changes in oil films affect the emergency resource scheduling decision making, the influence of the emergency response efforts on the dynamic motion of the oil films should also be taken into account. The emergency system has a high degree of uncertainty and significant time-varying characteristics, and the evolution of an oil spill accident itself interacts with the emergency logistics decision-making process, of which the interrelationship is shown in Fig. 1. Note that different from normal accidents, large-scale oil spills are treated as major accidents of catastrophic consequences. The emergency response to large-scale oil spills is often associated with a centralized decision making organization. It is under the command of the administrative department at a national/regional level to coordinate emergency resource scheduling of multiple resources and assign tasks of emergency operations to related departments and emergency forces.

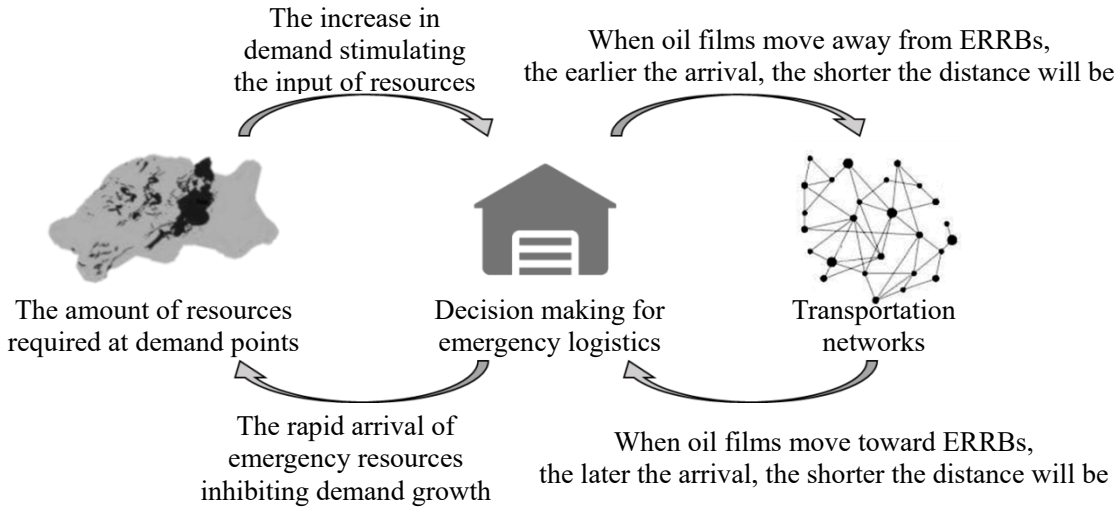

Fig. 1. The interrelationships in emergency logistics for oil spill accidents.

The proposed model aims to aid the centralized decision making organization: 1) to determine the ERRBs to constitute emergency fleets; 2) to plan the routes for emergency fleets from the ERRBs to the demand points considering time-varying demand and uncertain transportation networks; and 3) to allocate emergency resources and assign vessels to emergency fleets.

3.2 Dynamic motion of oil films

3.2.1 Diffusion process

Under the influence of tension, the size of the oil film area grows from small to large through diffusion. Fay (1969) proposed a scientific oil film diffusion model that divides the whole process into three stages according to the effects of various forces at different stages, comprehensively considering the effects of gravity, surface tension, inertial force and adhesion force. At present, this model is still widely used as a basis to develop mainstream oil spill prediction systems. After integrating the three-stage oil film diffusion model, Liu and Leendertse (1981) proposed an improved oil spill diffusion model as follows:

$$D = f(t,Q) = 0.61 \cdot [1.3 \cdot (\beta \cdot g \cdot Q)^{1/2} \cdot t + 2.1 \cdot (\frac{\beta \cdot g \cdot Q^2}{\sqrt{\nu_w}})^{1/3} \cdot t^{1/2} + 5.29 \cdot (\frac{\eta^2 \cdot t^3}{\rho_w^2 \cdot \nu_w})^{1/2}]^{1/2} \quad (1)$$

D is the oil film diameter; ρ_w is seawater density; ρ_0 is the oil density; β is simply a parameter, and $\beta = 1 - \rho_0 / \rho_w$; g is the acceleration of gravity; Q is the quantity of oil; ν_w is the viscosity coefficient; t is the time; and η is the net surface tension coefficient. In view of its reliability and feasibility, this paper adopts this model to reflect the oil spill diffusion process.

3.2.2 The drift process

The drift motion of oil films at sea is mostly affected by the geostrophic force, surface flow and sea surface wind (Zhang et al., 1991). The drift velocity can be determined by the following functions:

$$U_T = U_C + U_W \quad (2)$$

$$|U_W| = K \cdot |U_{10}| \quad (3)$$

U_T is the drift velocity of the oil film in the sea, which is obtained by adding the velocity of the ocean surface flow U_C to the drift velocity vector U_W; U_W is the drift velocity vector caused by U_{10} (i.e., the wind speed 10 meters above the sea); and K is the drift coefficient of the wind. The included angle α of U_W and U_{10} (as shown in Fig. 2) is the offset deflection angle (clockwise in the Northern Hemisphere), which is usually determined by Ekman's formula.

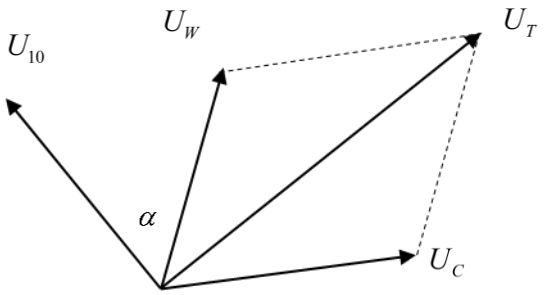

Fig. 2. Analysis diagram of the drift velocity of oil films.

3.3 Quantifying the value of ecological environmental loss

To evaluate the value of ecological environmental loss caused by the leakage of oil, chemicals and other toxic materials, researchers have put forward mature economic evaluation methods (Ando et al., 2004). These methods often require an extensive amount of data and take a long time to obtain an evaluated the value. Simplified formulas or computer models are therefore used to assess ecological damage. These types of simplified evaluation methods have the advantages of simplicity, low cost, small demand for information and easier operation in practice. The Florida formula, which is proven to be a fast and low-cost method for oil spill ecological damage assessment (Faass et al., 2010), is adopted and modified in Equation (4) to evaluate the ecological environmental loss value.

$$Dam = EK \cdot M \cdot SMA \cdot PC \tag{4}$$

Dam is the value of the ecological environmental loss; *EK* is the coefficient value of different ecological environments; *M* is the area of the contaminated ecological environment; *SMA* is the environmental sensitivity coefficient; and *PC* is the physicochemical coefficient of the pollution.

The area of the ecological environment contaminated in an oil spill accident is equal to that of the oil films presented. Given that the oil film diameter can be determined through Equation (1), Equation (4) can be transformed as follows:

$$Dam(t,Q) = \frac{\pi}{4} \cdot \left[f(t,Q) \right]^2 \cdot EK \cdot SMA \cdot PC \tag{5}$$

4 A methodology for optimizing emergency logistics for oil spill accidents at sea

This section introduces a new methodology for an efficient resource scheduling strategy for emergency logistics in oil spills that respects the constraints and specifics of oil spills. Our model is built with a capacity to cope with the complexity of the emergency response process, resulting from the time-varying demands of contaminated areas, the dynamic state of transportation networks at sea and the interrelationship between the changes in spilled oil films and emergency operations. It can also help ensure both emergency operation efficiency maximization and response cost minimization. In other words, our approaches focus on the trade-offs between responsiveness and the total response cost.

4.1 Assumptions

(1) Prior to making decisions regarding dynamic emergency logistics, the distribution of the demand points and the amount of spilled oil can be identified through advanced aerial monitoring technology and a geographic information system (GIS), and no new contaminated areas or spilled oil will be generated during the emergency response efforts.

(2) The external surroundings remain stable during the emergency response, so the oil film spreading rate is stable and the drift speed remains constant. Similarly, emergency vessel speed is set at a constant rate.

(3) In the case of a shortage of inventory or transportation capacity, the ERRBs can obtain timely support from suppliers and nearby ports without a time lag. The suppliers and ports have sufficient supplies and capacity to meet the replenishment needs of the ERRBs, but the cost for supplementary resources and vessels are higher than those of

ERRBs' own resources and vessels.

(4) The transportation and delivery of emergency resources shall be carried out by fleets. Different fleets follow diverse routes without interleaving intermediate nodes to transport and deliver emergency resources to each demand point. The fleet capacity can meet the demand for emergency resources at all demand points along the route at one time.

4.2 Notations and definitions

Sets and indexes

A Set of demand points, $a \in A = \{1, 2, \cdots, n\}$;

B Set of ERRBs, $b \in B = \{n+1, n+2, \cdots, n+m\}$;

V Set of all the nodes involved in the maritime emergency logistics networks, $V = A \bigcup B$;

R Set of emergency fleets, $r \in R = \{1, 2, \cdots, l\}$;

Time-varying parameters

$Dam(t, Q_a)$ Value of ecological environmental loss incurred at point a with Q_a tons of spilled oil at time t, $a \in A$;

$d_a(t)$ Quantity of emergency resources demanded by point a at time t, $a \in A$;

$dis_{ij}(t)$ Distance between node i and node j at time t, $i, j \in V$;

$g_a(t, Q_a)$ Growth rate of demand at point a with Q_a tons spilled oil at time t, $a \in A$;

Normal parameters

Q_a Quantity of spilled oil at point a, $a \in A$;

k_b Total number of emergency vessels equipped at ERRB b, $b \in B$;

q_b Quantity of emergency resources reserved by ERRB b, $b \in B$;

ek Efficiency of delivering emergency resources per vessel;

e_r Efficiency of delivering emergency resources by fleet r, $r \in R$;

v_j Drift velocity of node j ($j \in V$), if $j \in B$, $v_j = 0$;

vk Speed of emergency vessels;

qk Maximum cargo capacity per vessel;

ock Fixed operating cost of the emergency vessel owned by the ERRBs;

sck Fixed operating cost of supplementary emergency vessels from nearby ports;

ocq Unit consumption cost of self-owned emergency resources in the ERRBs;

scq Unit consumption cost of supplementary emergency resources from suppliers;

ct Transportation cost of the emergency vessel per nautical mile;

t_{rij} Duration of emergency fleet r from node i to node j, $r \in R$, $i, j \in V$;

t_{rj} Moment when emergency fleet r arrives at node j, $r \in R$, $j \in V$;

T_{ri} Moment when emergency fleet r is to leave node i for the next node, $r \in R$, $i \in V$;

$\hat{T}$ Time difference between the occurrence of the accident and the beginning of emergency operations;

Decision variables

u_{rb} 1, if emergency fleet r belongs to ERRB b, and 0 otherwise, $r \in R$, $b \in B$;

y_{rij} 1, if emergency fleet r travels from node i to node j, and 0 otherwise, $r \in R$, $i, j \in V$;

z_{ra} 1, if emergency fleet r is responsible for the transportation and delivery of emergency resources to point a, and 0 otherwise, $r \in R$, $a \in A$;

k_r Number of emergency vessels in emergency fleet r, $r \in R$;

q_r Total quantity of emergency resources allocated to emergency fleet r, $r \in R$.

4.3 Optimization model of emergency resource scheduling for oil spill accidents

4.3.1 Objective functions

Objective 1: Minimize the value of ecological environmental loss caused by oil spill pollution

This value is mainly determined by the oil film areas. We assume that oil films can be controlled in a timely manner after the delivery of emergency resources and the oil film areas will no longer be expanded. Therefore, when emergency fleet *r* has delivered emergency resources to point *a*, the area of the oil film at the point is no longer enlarged. In addition, there is a considerable time difference between the occurrence of an oil spill accident and the actual implementation of emergency measures. This paper focuses on the minimum value of ecological environmental loss caused by oil spills from the beginning of emergency operations. It does not take into consideration any environmental damage caused before the response begins. Therefore, based on Equation (5), objective 1 is formulated as follows:

$$\min \ Z_1 = \sum_{a\in A}\sum_{r\in R}\left[Dam(T_{ra}+\hat{T},Q_a) - Dam(\hat{T},Q_a)\right]\cdot z_{ra} \tag{6}$$

In Equation (6), $Dam(T_{ra}+\hat{T},Q_a)$ denotes the value of the ecological environmental loss at demand point *a* with Q_a tons spilled oil after the delivery of emergency resources, while $Dam(\hat{T},Q_a)$ denotes the value of ecological environmental loss at demand point *a* with Q_a tons spilled oil at the beginning of emergency operations.

Objective 2: Minimize the total cost of emergency logistics

The total cost generated in the process of emergency logistics mainly includes the fixed operation cost of emergency vessels, the resource consumption cost and the fleet travel cost. Specifically, the total cost consists of the following six components: the fixed operating cost of the emergency vessels owned by the ERRBs (*OCOV*), the fixed operating costs of the emergency vessels collected from the nearby ports (*OCSV*), the consumption cost of self-owned resources in the ERRBs (*CCOR*), the consumption cost of supplementary resources from suppliers (*CCSR*), the travel cost generated between the nodes of the networks (*TCN*), and the travel cost generated by oil film drift (*TCD*). The second objective function is therefore formulated as follows:

$$\min \ Z_2 = OCOV + OCSV + CCOR + CCSR + TCN + TCD \tag{7}$$

$$OCOV = \sum_{b\in B} ock \cdot \min\left\{ \sum_{r\in R} k_r \cdot u_{rb} \ , \ k_b \right\} \tag{8}$$

$$OCSV = \sum_{b\in B} sck \cdot \max\left\{ (\sum_{r\in R} k_r \cdot u_{rb} - k_b) \ , \ 0 \right\} \tag{9}$$

$$CCOR = \sum_{b\in B} ocq \cdot \min\left\{ \sum_{r\in R} q_r \cdot u_{rb} \ , \ q_b \right\} \tag{10}$$

$$CCSR = \sum_{b\in B} scq \cdot \max\left\{ (\sum_{r\in R} q_r \cdot u_{rb} - q_b) \ , \ 0 \right\} \tag{11}$$

$$TCN = \sum_{r\in R}\sum_{i\in V}\sum_{j\in V} ct \cdot vk \cdot t_{rij} \cdot y_{rij} \tag{12}$$

$$TCD = \sum_{r\in R}\sum_{i\in A} ct \cdot v_i \cdot \left(T_{ri} - t_{ri}\right) \cdot z_{ri} \tag{13}$$

4.3.2 Constraints of the multi-objective model

$$t_{rj} = \sum_{i\in V} (T_{ri} + t_{rij}) \cdot y_{rij} \ , \ \ \forall r \in R \ , \ \ \forall i, j \in V \tag{14}$$

$$t_{rij} = F(T_{ri}) \ , \ \ \forall r \in R \ , \ \ \forall i, j \in V \tag{15}$$

Constraint (14) defines the moment when emergency fleet *r* reaches node *j*. Constraint (15) defines the travel time of emergency fleets between nodes, and $F(T_{ri})$ is explained below in reference to Equation (32).

$$T_{ri} = 0 \ , \forall r \in R \ , \forall i \in B \tag{16}$$

$$\int_0^{t_{ri}+\hat{T}} g_i(t,Q_i)\mathrm{d}t = \int_{t_{ri}+\hat{T}}^{T_{ri}+\hat{T}} \left(e_r - g_i(t,Q_i)\right)\mathrm{d}t \,, \forall r \in R, \quad \forall i \in A \tag{17}$$

Constraints (16) and (17) define the moment when emergency fleet *r* leaves node *i*, where $g_i(t,Vo_i)$ needs to be determined according to the specific law of emergency resource consumption.

$$d_i(t)=\int_0^t g_i(t,Q_i)\mathrm{d}t = \pi \cdot f(t,Q_i), \quad \forall i \in A \tag{18}$$

Constraint (18) represents the time-varying demand at demand point *i* with Q_i tons spilled oil. When emergency resources are oil booms, the amount of demand for emergency resources at the demand point can be expressed by the perimeter of the oil film, so it can be formulated based on Equation (1).

$$e_r = k_r \cdot ek \,, \forall r \in R \tag{19}$$

$$\left\lceil \frac{\sum_{i \in A} d_i(T_{ri}) \cdot z_{ri}}{qk} \right\rceil = k_r \,, \forall r \in R \tag{20}$$

Constraint (19) defines the efficiency of delivering the emergency resource (i.e., installing oil booms) of emergency fleet *r*. Constraint (20) stipulates that the transportation capacity of emergency fleet *r* is just enough to meet the total demand for emergency resources at all demand points for which emergency fleet *r* is responsible, to ensure that the transportation capacity of each emergency vessel is fully utilized.

$$\sum_{j \in A} y_{rij} = u_{ri} \,, \forall r \in R \,\,, \forall i \in B \tag{21}$$

$$\sum_{r \in R} y_{rij} = 0 \,, \forall i, j \in B \tag{22}$$

Constraint (21) stipulates that emergency fleet *r* owned by ERRB *i* has only one transportation route and that the starting point of the route can only be ERRB *i*. Constraint (22) means that emergency fleet *r* will not travel between ERRBs.

$$\sum_{i \in V} y_{rij} - \sum_{i \in V} y_{rji} = 0 \,, \forall r \in R \,, \forall j \in V \tag{23}$$

$$\sum_{i \in V} y_{rij} + \sum_{i \in V} y_{rji} \le 2 \,, \forall r \in R \,, \forall j \in V \tag{24}$$

Constraint (23) represents the conservation of the emergency fleet flow. Constraint (24) means that each node allows emergency fleet *r* to pass no more than once to eliminate the route sub-loop and avoid the formation of any circular route that does not pass ERRBs.

$$\sum_{r \in R} z_{ri} = 1 \,, \forall i \in A \tag{25}$$

Constraint (25) means that there is one and only one emergency fleet to deal with each demand point.

$$y_{rij} \cdot \left(t_{rj} - t_{ri}\right) \ge 0 \,, \forall r \in R \,, \forall i, j \in V \tag{26}$$

Constraint (26) indicates that the nodes in the transportation route of emergency fleet *r* are in sequence.

$$u_{ri} = \{0,1\}, \quad \forall r \in R \,\,, \forall i \in B \tag{27}$$

$$y_{rij} = \{0,1\} \,, \forall r \in R \,, \forall i, j \in V \tag{28}$$

$$z_{ri} = \{0,1\}, \quad \forall r \in R \,\,, \forall i \in A \tag{29}$$

The binary integer constraints for the decision variables are given in Constraints (27)–(29).

In addition, the oil films are drifting due to the influence of the external forces at sea. When emergency fleet *r* is to leave node *i* and sails to the next node *j*, the travel distance changes due to the dynamic change of the oil film areas at point *i* and *j*. Here, we use a mathematical derivation to determine the travel time of emergency fleets between different nodes. The positions of the nodes at sea are shown in Fig. 3, where a_i is the position of node *i*, a_j is

that of node j and a_j^* is where emergency fleet r meets node j.

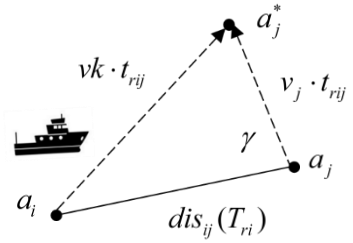

Fig. 3. Stroke diagram of the dynamic route.

Based on the cosine theorem, the following equation is formulated:

$$\begin{aligned} &\left(vk \cdot t_{rij}\right)^2 = dis_{ij}^2(T_{ri}) + \left(v_j \cdot t_{rij}\right)^2 - 2 \cdot dis_{ij}(T_{ri}) \cdot v_j \cdot t_{rij} \cdot \cos\gamma \\ &\Rightarrow t_{rij} = \frac{-v_j \cdot dis_{ij}(T_{ri}) \cdot \cos\gamma \pm dis_{ij}(T_{ri}) \cdot \sqrt{vk^2 - v_j^2 \cdot \sin^2\gamma}}{vk^2 - v_j^2} \end{aligned} \tag{30}$$

According to Equation (30), the following speed constraint shall be met when emergency fleet r is able to meet point j:

$$vk^2 - v_j^2 \cdot \sin^2\gamma \geq 0 \Rightarrow vk \geq v_j \cdot \sin\gamma \tag{31}$$

Therefore, the function of the travel time between nodes is formulated as follows:

$$t_{rij} = F(T_{ri}) = \frac{-v_j \cdot dis_{ij}(T_{ri}) \cdot \cos\gamma + dis_{ij}(T_{ri}) \cdot \sqrt{vk^2 - v_j^2 \cdot \sin^2\gamma}}{vk^2 - v_j^2}, \quad \forall r \in R, \quad \forall i, j \in V \tag{32}$$

5 Solution procedure

In the context of the emergency response efforts to oil spills, searching for an immediate and ideal solution is crucial when facing a large-scale oil spill accident. It is worth noting that it is useless and intractable to solve the proposed model with a number of time-varying parameters and constraints via the off-the-shelf solvers and conventional heuristic algorithms. After the comprehensive consideration of the characteristics of the proposed model and the candidate algorithms, particle swarm optimization (PSO) is considered as the heuristic framework of the improved algorithm in this paper.

5.1 Motivations for the PSO algorithm

According the reviewed literature, the solution methods (in Column 5 of Table 1) can be grouped into the exact approaches and the heuristic algorithms. Most studies tend to adopt the exact approaches which utilize the off-the-shelf solvers, such as CPLEX, LINGO and so on, to solve the optimization problems. The models in these studies are all mono-objective models or mono-objective models transformed from multi-objective ones, because the exact approaches cannot directly solve multi-objective optimization problems. Although for small or medium scale case, optimization problems can be well solved by off-the-shelf solvers like CPLEX, the heuristic algorithms are more popular than the exact approaches to solve the optimization model with an increasing complexity (Cao et al., 2018). Based on the characteristics of the proposed model in this paper, the heuristic algorithm is considered as the solution method.

As shown in Table 1, both the non-dominated sorting genetic algorithm-II (NSGA-II) and PSO are in the majority of the heuristic algorithms used for emergency logistics optimization problems. Although some other state-of-the-art algorithms have been demonstrated to be more efficient on benchmark problems, the application of these algorithms in the field of emergency logistics has been less explored and the computational performance of these algorithms lacks empirical case verification (Zheng et al., 2015). The reliability of the calculation results can be better guaranteed by adopting the frequently-used and recognized solution algorithms (i.e., NSGA-II and PSO). Based on the comprehensive consideration of the characteristics of the proposed model and the candidate algorithms, instead of NSGA-II, PSO is determined as the

heuristic framework of the improved algorithm to solve the proposed model in this paper. The specific reasons are listed as follows.

First, empirical studies have shown that the PSO algorithm has a much higher efficiency in convergence to desirable optima than many other heuristic algorithms including the genetic algorithm (Eberhart et al., 2001). Meanwhile, the PSO algorithm can search a hyper dimensional space within a reasonable runtime, which is relatively applicable to the proposed model. In addition, some of the reviewed studies which aim to address the similar problem to this paper demonstrate that the PSO algorithm has the advantages on solution quality and efficiency (Huang et al., 2020; Ghasemi et al., 2019; Song et al., 2017).

Second, there are complex genetic operations in the NSGA-II algorithm, such as selection, crossover, mutation and so on. Compared to the NSGA-II algorithm, the PSO algorithm can avoid these cumbersome operations and is relatively straightforward, and is more suitable to be implemented for solving scheduling problems because of its simplicity and high convergence (Ye et al., 2019).

Third, the proposed model in this paper cannot be solved directly by neither the off-the-shelf solvers nor the conventional heuristic algorithms, due to the dynamic motion of the oil films which is represented by the time-varying parameters. The specific reason is explained in Section 5.3.3. Hence, there is a must to develop an improved algorithm to effectively solve the proposed model. Since the PSO algorithm has the advantages of high compatibility and simplicity, it has a wide extension with other methods (Tian et al., 2018). Of course, there are plenty of achievements of the modified algorithms based on PSO that can be leveraged and extended, which strengthens its ability to deal with complex real-world problem regarding oil spills.

5.2 Conventional PSO

PSO is an intelligent optimization method proposed by Kennedy and Eberhart (1995). In this algorithm, the solutions to an optimization problem are regarded as particles in the search space, and the optimal solution is obtained by continuous iteration. During the iteration process, each particle updates its own position and generates a new particle for the next generation by tracking the individual optimal position and the global optimal position. Let the number of particles in the population be N, where the velocity and position of the *i*-th particle after the τ-th iteration in D-dimensional space are $v_i^\tau = \left[v_{i1}^\tau, v_{i2}^\tau, \cdots, v_{iD}^\tau \right]$ and $x_i^\tau = \left[x_{i1}^\tau, x_{i2}^\tau, \cdots, x_{iD}^\tau \right]$ respectively. In conventional PSO, the updated functions for the velocity and positions of the particles are formulated as follows:

$$v_{id}^{\tau+1} = \omega \cdot v_{id}^\tau + c_1 \cdot r_1 (p_{id}^\tau - x_{id}^\tau) + c_2 \cdot r_2 (p_{gd}^\tau - x_{id}^\tau)$$

$$v_{id}^{\tau+1} = \begin{cases} v_{\max} \ , \ if \ v_{id}^{\tau+1} > v_{\max} \\ -v_{\max} \ , \ if \ v_{id}^{\tau+1} < -v_{\max} \end{cases} \tag{33}$$

$$x_{id}^{\tau+1} = x_{id}^\tau + v_{id}^{\tau+1} \tag{34}$$

ω is the inertial weight and $\omega = \omega_{\max} - (\omega_{\max} - \omega_{\min}) \cdot \frac{\tau}{\mathrm{T}}$, where $\omega_{\max}$ and $\omega_{\min}$ are the maximum and minimum weights, respectively. τ is the current number of iterations, and T is the maximum number of iterations. c_1 and c_2 are the learning factors, which are usually set as $0 < c_1, c_2 < 2$ to ensure algorithm convergence. r_1 and r_2 are random numbers that are evenly distributed between 0 and 1. $v_{\max}$ is the limitation of the maximum speed, which determines the search accuracy of the particles in the feasible region. The optimal solution obtained by particle *i* after the τ-th iteration is the individual optimal solution $Pbest_i$, and its position is $p_i^\tau = [p_{i1}^\tau, p_{i2}^\tau, \cdots, p_{iD}^\tau]$. Moreover, the optimal solution found for the whole population is the global optimal solution $Gbest$, and its position is $p_g^\tau = [p_{g1}^\tau, p_{g2}^\tau, \cdots, p_{gD}^\tau]$.

5.3 Operations of an improved multi-objective particle swarm optimization (IMPSO) algorithm

In practice, decision makers need high-quality decision support to develop emergency resource scheduling schemes. To enhance the search capability of the improved algorithm, the niche sharing mechanism is introduced in the heuristic framework. Moreover, because of the innovative time-varying characteristics of the proposed model, the conventional heuristic algorithms are unable to solve it. Therefore, the iterative dynamic programming is embedded in the improved algorithm to effectively resolve the calculation difficulties caused by the time-varying parameters.

5.3.1 Introduction of the niche sharing mechanism

The key issue in applying the PSO algorithm to solve the multi-objective optimization problem is the selection and preservation of p_i^τ and p_g^τ. In the literature, these values are often randomly selected (Zhang et al., 2017a). When the particles in an area of the external archive are too dense, the probability that these particles will be selected as the global optimal position greatly increases. Thus, the particles in the whole iteration process are guided to move toward this region so that the local convergence and prematurity of the calculation easily occur. To avoid such a problem, we use the niche sharing mechanism (Jebari et al., 2013) to select the global optimal position.

According to the niche sharing mechanism, the fitness of particle x_i in the external archive is defined as follows:

$$F_i = \frac{1}{S_i},\ i = 1, 2, \cdots, N_s \tag{35}$$

N_s is the total number of particles in the current external archive, and S_i is the sharing degree of particle x_i, which can be formulated as follows:

$$S_i = \sum_{j=1}^{N_s} f_{sh}(d_{ij}),\ i = 1, 2, \cdots, N_s \tag{36}$$

$f_{sh}(d_{ij})$ is the shared function between particles x_i and x_j, and it represents the degree of closeness between them. It is defined as follows:

$$f_{sh}(d_{ij}) = \begin{cases} 1 - (\dfrac{d_{ij}}{\sigma_{share}})^{\alpha}, & 0 \le d_{ij} < \sigma_{share} \\ 0, & d_{ij} \ge \sigma_{share} \end{cases} \tag{37}$$

α is the parameter that controls the shape of the shared function, which is usually set as 1 or 2. σ_{share} is the shared distance. d_{ij} is the distance between particles x_i and x_j, which is usually measured by the Euclidean distance as follows:

$$d_{ij} = \left\| x_i - x_j \right\| = \sqrt{\sum_{d=1}^{D} (x_{id} - x_{jd})^2} \tag{38}$$

The greater the sharing degree of the particle is, the smaller the fitness of the particle in the external archive, and vice versa. In the iteration of PSO, this method can be used to evaluate the fitness of the particles in the external archive, and then to select the particle as the global optimal position following the roulette selection principle. This method can effectively reduce the probability of similar particles being selected in the iteration, to ensure the diversity of particles and avoid the occurrence of local convergence and prematurity.

5.3.2 Particle coding operations

In this paper, we adopt decimal particle coding to represent the solutions in IMPSO to solve the particular multi-objective location-routing problem. Each encoding sequence denotes an emergency resource scheduling scheme for oil spill accidents. Each particle is represented by x_i^τ, as defined in Section 5.1. Specifically, the encoding sequence of each particle consists of three sub-strings as shown in Equation (39), and the total number of the code bits is D.

$$x_i^\tau = \{\underbrace{(x_{i11}^\tau, x_{i12}^\tau, \cdots, x_{i1n}^\tau)}_{x_{i1}^\tau}, \underbrace{(x_{i21}^\tau, x_{i22}^\tau, \cdots, x_{i2n}^\tau)}_{x_{i2}^\tau}, \underbrace{(x_{i31}^\tau, x_{i32}^\tau, \cdots, x_{i3h}^\tau)}_{x_{i3}^\tau}\} \tag{39}$$

The encoding sequence of the particle is a D-dimensional vector with each bit randomly generated between 0 and 1. The number of code bits in sub-strings x_{i1}^τ and x_{i2}^τ is n, the same as that of the demand points. Sub-string x_{i3}^τ is a sequence with *h* bits, the same number as that of emergency fleets. Thus, each encoding sequence of the particle (given by $n + n + h$=D) is a D-dimensional vector.

In the calculation process, the random number in sub-string x_{i1}^τ will be multiplied by *h* and rounded up, which means that the corresponding emergency fleet is responsible for the transportation and delivery of emergency resources to the demand point of this bit. Similarly, the codes of sub-string x_{i3}^τ will be converted into random numbers from 1 to *m* (the total number of ERRBs), which means that the emergency fleet of each coding bit is owned by the corresponding ERRB. The codes in sub-string x_{i2}^τ display the rank of the decimals of each coding bit in the sequence in an order from small to large. In other words, the codes of sub-string x_{i2}^τ will be converted into random numbers from 1 to *n*, and every number between 1 and *n* will occur once and only once.

Sub-strings x_{i1}^τ and x_{i2}^τ together make the routing decisions for each emergency fleet. The fleet denoted by the first bit in sub-string x_{i1}^τ is responsible for the demand point denoted by the first bit in sub-string x_{i2}^τ, the fleet denoted by the second bit in sub-string x_{i1}^τ is responsible for the demand point denoted by the second bit in sub-string x_{i2}^τ, and so forth.

Sub-string x_{i3}^τ makes the location decisions for each fleet's origin ERRB, that is, the ERRB denoted by the first bit in sub-string x_{i3}^τ is responsible for constituting the first fleet, the ERRB denoted by the second bit in sub-string x_{i3}^τ is responsible for constituting the second fleet, and so forth.

5.3.3 Iterative dynamic programming for the variables affected by time-varying parameters

Through the abovementioned particle coding operations, we can make decisions on the selection of ERRBs and route planning in emergency logistics for each emergency fleet. However, the encoding sequence does not involve the variables of emergency resource allocation and vessel dispatching, which are directly affected by the time-varying parameters.

The proposed model in this paper cannot be solved directly by the conventional heuristic algorithms, because there are a number of time-varying parameters in the objective function and constraints. As we all know, the candidate solutions in the conventional heuristic algorithms, such as chromosomes in NSGA-II and particles in PSO, cover the values of all the decision variables related to the problem to be solved, and all of these values are determined before the iterative calculation of the heuristic algorithms. Due to the dynamic motion of the oil films, the demand of emergency resources for oil spills and the travel distance of the emergency fleets between the nodes in the associated transportation networks cannot be determined in advance, which means that the values of the corresponding time-varying parameters cannot be obtained in advance. In the proposed model, there is strong coupling between the time-varying parameters and the decision variables. When the decision variables are determined, the values of the time-varying parameters can be obtained according to the calculation logic of the proposed model. In turn, the obtained time-varying parameters will impose constraints on the decision variables, which directly affects the decisions on emergency resource allocation and vessel dispatching. Herein, the conventional heuristic algorithm can make use of the preset values of the decision variables for emergency resource allocation and vessel dispatching to neither precisely meet the time-varying constraints nor determine the exact values of the time-varying parameters. Therefore, the improved algorithm only uses the decision variables within the candidate solutions to make the decisions without time-varying properties, such as locating the emergency resource reserved bases and planning

the routes for the emergency fleets. As for the decision making for emergency resource allocation and vessel dispatching, it is realized by the iterative dynamic programming embedded in the proposed algorithm, which adjusts the relevant decision variables to meet the constraints imposed by the time-varying parameters, so as to coordinate the interrelationship between the changes in spilled oil films and emergency operations. Dynamic programming formulations can be created in various ways, depending on the rules of the operation of the process being modeled (Berman, et al., 2001). The iterative dynamic programming procedure for the abovementioned variables is described as follows:

Step 1: Determine the number of vessels allocated to fleet r ($\forall r \in R$) according to the initial state of the oil spill distribution as follows:

$$\left\lceil \frac{\sum_{i \in A} d_i(\hat{T}) \cdot z_{ri}}{qk} \right\rceil = k_r, \quad \forall r \in R \tag{40}$$

Step 2: By putting k_r into the dynamic optimization model, the total demand of the demand points $\sum_{i \in A} d_i(T_{ri}) \cdot z_{ri}$ ($\forall r \in R$), which are in the charge of emergency fleet r, can be obtained. The value of T_{ri} can be obtained by equation derivation of Constraints (14)-(19).

Step 3: Subtract the total capacity of the fleet from the total demand of resources to obtain the difference Δ, as follows:

$$\Delta = \sum_{i \in A} d_i(T_{ri}) \cdot z_{ri} - q_r = \sum_{i \in A} d_i(T_{ri}) \cdot z_{ri} - k_r \cdot qk, \quad \forall r \in R \tag{41}$$

Step 4: Adjust the number of ships assigned to the fleet according to the difference, as follows:

$$\begin{cases} k_r \leftarrow k_r + \left\lceil \dfrac{\Delta}{qk} \right\rceil, \ \Delta \geq 0, \ \forall r \in R \\ k_r \leftarrow k_r + \left\lfloor \dfrac{\Delta}{qk} \right\rfloor, \ \Delta < 0, \ \forall r \in R \end{cases} \tag{42}$$

Step 5: Terminate the iterative dynamic programming procedure if Constraint (20) is met, and then variables such as k_r and q_r ($\forall r \in R$, $\forall i, j \in V$) can be obtained; otherwise, return to Step 2.

5.4 IMPSO procedure

The steps of the IMPSO are shown in Fig. 4 and are described as follows.

Step 1: Initialize the population of particles. The initial position x_i^0 and the initial velocity v_i^0 of N particles are randomly generated. The optimal position of the initial individual of the particle is $p_i^0 = x_i^0$. The external archive is empty.

Step 2: Calculate the fitness values of the particles. By converting the coding information of each particle into decision variables and substituting them into the optimization model, the corresponding multi-objective function values can be simultaneously obtained via the iterative dynamic programming and then saved as the fitness value of the particle.

Step 3: Select the non-dominated solutions. According to the fitness value of each particle, the non-dominated solutions can be identified on the basis of Pareto dominance.

Step 4: Update and maintain the external archive. The non-dominated solutions of the current population are entered into the external archive, and the particles in the external archive are sorted on the basis of Pareto dominance. Then, eliminate the dominated particles and only keep the non-dominated particles. If the number of particles in the external archive exceeds the set capacity, then the excess particles will be removed in an order from small to large based on the niche fitness value until the number meets the set capacity.

Step 5: Judge the termination condition. Stop the procedure and obtain the calculation results if the iteration τ is equal to T (maximum of iteration times); otherwise, $\tau \leftarrow \tau + 1$ and continue to Step 6.

Step 6: Determine the global optimal position p_g^τ and the individual optimal position p_i^τ. According to Equation (35), the niche fitness values of the particles in the external archive can be determined. On this basis, the particle as the global optimal solution is selected through roulette selection and its position is considered as the global optimal position p_g^τ. Simultaneously, compare particle x_i^τ with $p_i^{\tau-1}$, and select the non-dominated particle as the optimal position p_i^τ of the current individual.

Step 7: Update the velocity and position of the particles. According to Equations (33) and (34), the particle velocity and position in the population can be updated.

Step 8: Repeat Steps 2-5 to obtain the newly generated external archive and then check the termination condition.

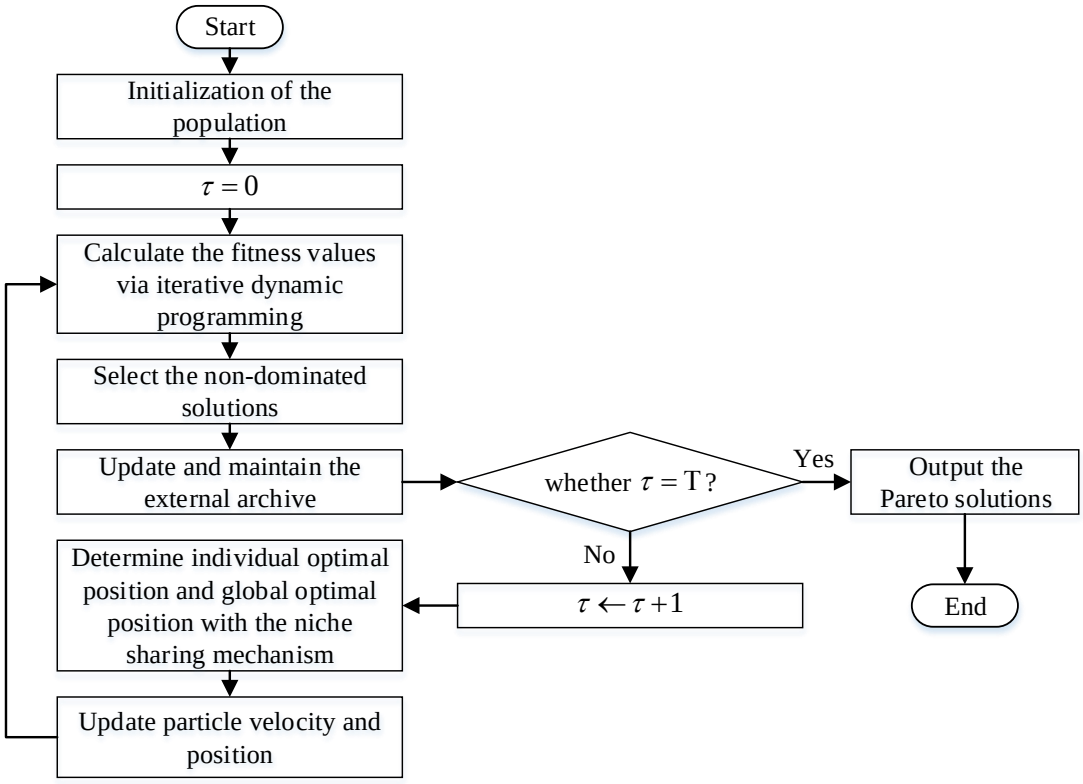

Fig. 4. The flow chart of IMPSO.

5.5 Ideal option for Pareto solutions

The selection of Pareto solutions is essentially a question as to how to weigh the importance of multiple objectives. If the comparison and selection are based on the market principle and rationality, then the common desire of decision makers is to obtain high-quality products at a lower price, that is, to obtain high cost performance. Through the distribution of the Pareto frontier, it can be observed that the Pareto distribution characteristics exhibit a specific trend, and most of the distribution is uneven, which means that there are different rates of change and sensitivity, from which important information similar to cost performance can be mined (Wang et al., 2018). On this basis, we adopt an alternative solution based on the cost performance method to select the ideal option from Pareto non-dominated solutions.

(1) Mean variability: this refers to the mean value of the slope of the line between any point (except the endpoint) and the adjacent two points in the Pareto frontier based on the objective function values. Let Z_1^s and Z_2^s represent the values of the objective functions of the non-dominated Pareto solution numbered s ($s = 2,3,\cdots,S-1$). Without loss of generality, the points of the Pareto frontier are numbered from small to large according to the values of the cost

objective function. The mathematical definition of the mean variability of the Pareto solution numbered *s* for the two objective functions is defined as follows:

$$k_1^s = \frac{1}{2} \cdot \left(\frac{Z_2^s - Z_2^{s-1}}{Z_1^{s-1} - Z_1^s} + \frac{Z_2^{s+1} - Z_2^s}{Z_1^s - Z_1^{s+1}} \right), \quad s = 2,3,\cdots,S-1 \tag{43}$$

$$k_2^s = \frac{1}{2} \cdot \left(\frac{Z_1^{s-1} - Z_1^s}{Z_2^s - Z_2^{s-1}} + \frac{Z_1^s - Z_1^{s+1}}{Z_2^{s+1} - Z_2^s} \right), \quad s = 2,3,\cdots,S-1 \tag{44}$$

(2) In particular, for the endpoint (s=1 or S), the mean variability of the two objective functions is defined as follows:

$$k_1^1 = \frac{1}{2} \cdot \frac{Z_2^2 - Z_2^1}{Z_1^1 - Z_1^2} \tag{45}$$

$$k_2^1 = \frac{1}{2} \cdot \frac{Z_1^1 - Z_1^2}{Z_2^2 - Z_2^1} \tag{46}$$

$$k_1^S = \frac{1}{2} \cdot \frac{Z_2^S - Z_2^{S-1}}{Z_1^{S-1} - Z_1^S} \tag{47}$$

$$k_2^S = \frac{1}{2} \cdot \frac{Z_1^{S-1} - Z_1^S}{Z_2^S - Z_2^{S-1}} \tag{48}$$

(3) Sensitivity ratio: this refers to the ratio of the values of the two kinds of mean variability to the values of the corresponding objective functions and is defined as follows:

$$\delta_l^s = \frac{k_l^s}{Z_l^s}, \quad s = 1,2,\cdots,S, \quad Z_l^s \neq 0, \quad \forall l \in \{1,2\} \tag{49}$$

(4) The above definition indicates that the value of the sensitivity ratio reflects the sensitivity of the mean variability of the objective function value relative to the unit value of the objective function. To facilitate the next comparison, the sensitivity ratio must be standardized as follows:

$$\varepsilon_l^s = \frac{\delta_l^s}{\sum_{s=1}^{S} \delta_l^s}, \quad s = 1,2,\cdots,S, \quad \forall l \in \{1,2\} \tag{50}$$

(5) Pareto dominance based on sensitivity ratio: if the sensitivity ratios of solution x_i are at least equal to those of x_j, and better than at least one of those of x_j, then solution x_i dominates solution x_j (denoted $x_i \succ x_j$). In formal terms, $x_i \succ x_j$ can be defined as follows:

$$(\forall l \in \{1,2\}, i, j \in \{1,2,\cdots,S\}, \ \varepsilon_l^i \geq \varepsilon_l^j) \wedge (\exists l \in \{1,2\}, i, j \in \{1,2,\cdots,S\}, \varepsilon_l^i > \varepsilon_l^j) \tag{51}$$

(6) Skewness based on sensitivity ratio: this reflects the degree of preference for different objectives, and its value ranges between 0 and 1. w_1^s and w_2^s are the skewness of the Pareto non-dominated solution numbered *s* based on the sensitivity ratio to the values of the objective functions Z_1 and Z_2, respectively. It can be formulated as follows:

$$w_l^s = \frac{\varepsilon_l^s}{\varepsilon_1^s + \varepsilon_2^s}, \quad s \in S^*, \quad \forall l \in \{1,2\} \tag{52}$$

where S^* is the set of Pareto non-dominated solutions based on the sensitivity ratio.

As optimization objectives are often contradictory, there is an associated trade-off. When w_1^s is the largest, the corresponding Pareto non-dominated solution is the strongly biased solution for the objective function Z_1, and vice versa. Therefore, w_1^s and w_2^s reflect the degree of preference of Pareto non-dominated solutions related to different optimization objectives. In conclusion, the Pareto non-dominated solution set based on the sensitivity ratio not only has a smaller range but also provides decision makers with more convenient quantitative indexes for weighing and comparing. Decision makers need only to clarify their preference to efficiently select an ideal option, and need not be concerned with the irrationality due to the subjectively assigned weight coefficients.

6 An application of the proposed methodology

6.1 Test case

The test case involves emergency logistics distribution for a major oil spill accident in the Bohai Bay, China. The parameters are determined prior to the route planning, configuration of emergency vessels and resource allocation. Because the data on the oil spill accident have not yet been fully released by the government, we manually collect and analyze data using the information provided by the local maritime bureau and use them to verify the model and algorithm. The corresponding parameters are set as follows.

(1) Demand information. Emergency operations begin six hours ($\hat{T}$) after the occurrence of the accident. Aerial reconnaissance by aircraft reveals that a large and dispersed oil film area forms at sea. According to the characteristics of the oil film in different areas, the analysis of emergency resources shows that there are 24 points with thick oil films in need of oil booms to control oil diffusion, as shown in Fig. 5.

(2) Oil films. There are two different drift velocities in the contaminated area of the sea under the action of two different currents. Some oil films drift to the south by east 37° at a speed of 1.8 kn. The other films drift to the north by west 24° at a speed of 1.2 kn. The relevant information on the quantity, position and drift velocity of the oil spilled at each demand point is shown in Table 1.

(3) ERRBs. There are three ERRBs near the contaminated area, namely, Dalian, Yantai and Weihai. The information related to emergency resources such as the resource inventory, resource consumption cost and vessel configuration of each ERRB is shown in Table 2.

(4) Vessels. To simplify the analysis, all the emergency vessels are treated as the same type and have the same performance, the details of which are shown in Table 3. For the emergency response, 6 emergency fleets are expected to be set up for the transportation and delivery of emergency resources.

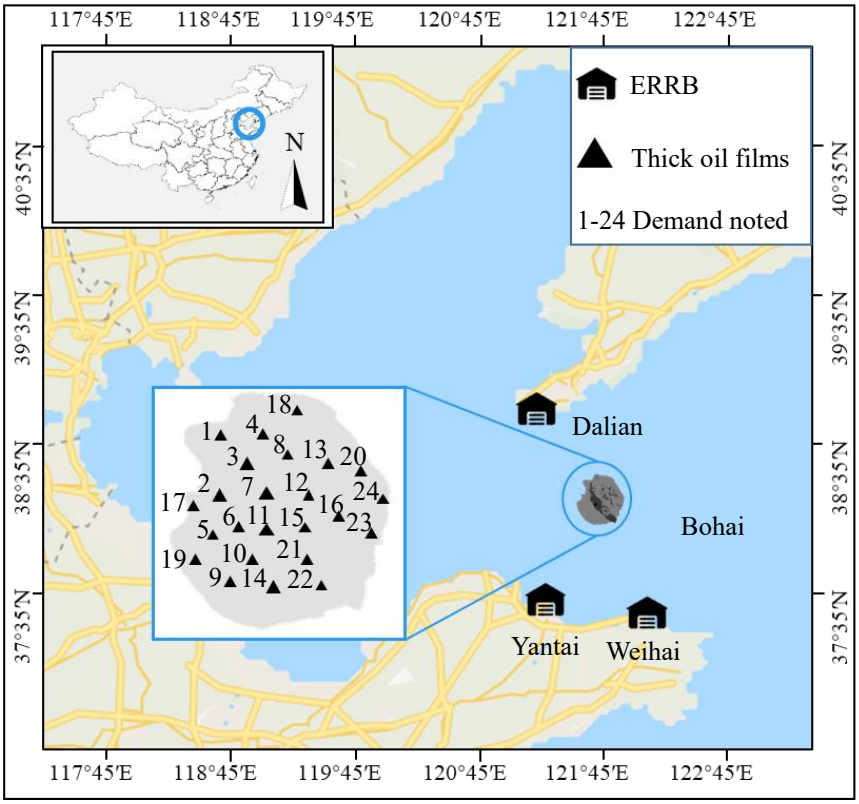

Fig. 5. Distribution of the demand points.

Table 1

Data of oil films at the demand points.

No.	Oil quantity (t)	Coordinates (E/N)	Velocity (kn)	No.	Oil quantity (t)	Coordinates (E/N)	Velocity (kn)
1	50	121.7357 /38.3818	1.8	13	35	121.9271 /38.3415	1.8
2	126	121.7334 /38.2854	1.2	14	153	121.8176 /38.1487	1.2
3	148	121.7913 /38.3352	1.8	15	62	121.8797 /38.2426	1.8
4	40	121.8205 /38.3853	1.8	16	52	121.9417 /38.26	1.8
5	98	121.7095 /38.2357	1.2	17	68	121.6773 /38.2756	1.2
6	67	121.7598 /38.2482	1.2	18	72	121.8811 /38.4229	1.8
7	154	121.8167 /38.2885	1.8	19	56	121.6718 /38.1985	1.2
8	78	121.8535 /38.3538	1.8	20	92	121.9955 /38.3334	1.8
9	36	121.7318 /38.158	1.2	21	58	121.8772 /38.1948	1.2
10	64	121.773 /38.1922	1.2	22	86	121.9027 /38.1563	1.2
11	162	121.811 /38.2326	1.2	23	47	122.0012 /38.2346	1.8
12	58	121.8893 /38.2979	1.8	24	83	122.0316 /38.2886	1.8

Table 2
Data of the ERRBs.

Name of ERRBs (No.)	Coordinates (E/N)	Number of equipped vessels	Oil booms reserved (m)	Unit cost of the self-owned (m/CNY)	Unit cost of replenishment (m/CNY)
Dalian (25)	121.1333 /38.75	42	31,500	8	12
Yantai (26)	121.396 /37.548	48	27,500	8	12
Weihai (27)	122.202 /37.452	35	25,800	8	12

Table 3
Data of the emergency vessels.

Speed (kn)	Capacity (m)	Delivery rate (m/h)	Operation cost of the self-owned (CNY)	Operation cost of the lease (CNY)	Unit transport cost (CNY/n mile)
12	600	200	3500	5000	20

6.2 Performance of the IMPSO and NSGA-II algorithms

The IMPSO described in Section 5 is programmed using MATLAB 2016b, and all the numerical experiments are carried out on the same computer with a 3.6 GHz i3-9100F processor, 8 GB RAM, and a 64-bit Windows 10 ultimate operation system. The length of the encoding sequence in the IMPSO is 54. With considerable research data, the appropriate values of the

control variables are determined empirically as follows: N=50, ω_{max} =0.9, ω_{min} =0.4, $c_1 = c_2 = 1.49445$, K=300, δ_{share} =2.9. To investigate the performance of IMPSO, it is compared with the established NSGA-II which has been accepted as one of the most popular and widely used algorithms for solving multi-objective emergency logistics problems (Ghasemi et al., 2019). In order to ensure the objectivity and validity of the comparison results, the parameter setting of the two algorithms is as consistent as possible. For NSGA-II, the population size is 50. The maximum iteration is set to 300. The crossover rate is set to 0.8 and the mutation rate is set to 0.02. Since the problem discussed is NP-hard, approximate solutions are recommended. To find the approximate solutions to the problem, ten runs are performed for the test case with both the IMPSO and NSGA-II algorithms, and the obtained Pareto fronts are shown in Fig. 6.

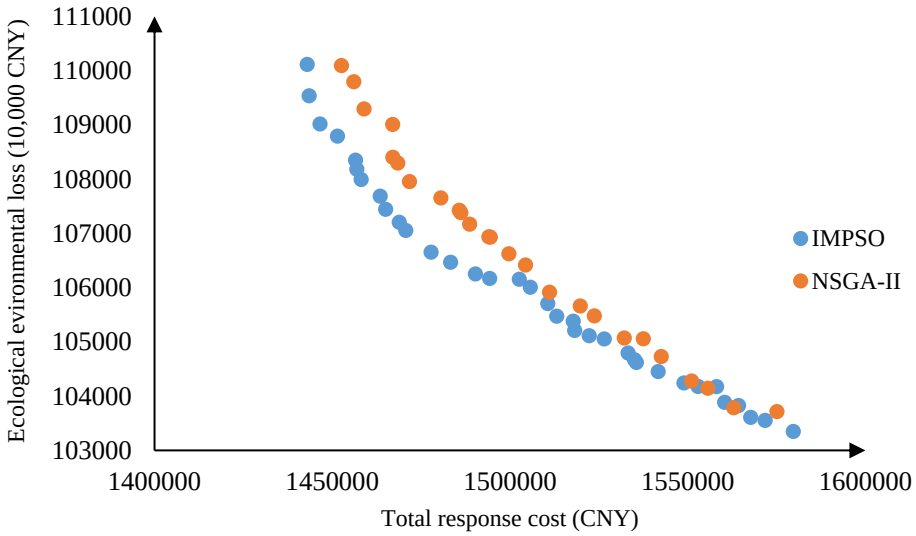

Fig. 6. Comparison between IMPSO and CMPSO.

6.2.1 Performance metrics

Through Fig. 6, the advantage of the IMPSO algorithm in accuracy and diversity can be directly observed. To further compare the performance of the two algorithms, three frequently-used metrics are adopted as follows: 1) spacing metric (SM), which calculates the standard deviation of the distance among solutions of the Pareto front and measures the uniformity of the spread of the non-dominated solutions (Ghasemi et al., 2019); 2) mean ideal distance (MID), which shows the closeness between the Pareto solutions and the ideal point, and is commonly used for a minimization problem with two objectives (Rashidnejad et al., 2018); 3) quantity metric (QM), which is the number of non-dominated solutions produced by an algorithm and reflects its ability to find feasible solutions (Rezaei et al., 2020).

Both IMPSO and NSGA-II are run for ten times and then their performance is compared against each other in terms of the aforementioned metrics (i.e., SM, MID and QM) and the required CPU time in seconds which reflects the computation time. Table 4 contains a comparison between performances of IMPSO and NSGA-II algorithms. The last row in the table shows the average (Avg) of the values for these four metrics in ten replications. Specifically, SM aims to measure how spread the non-dominated solutions in the entire region. A small value of SM means that the members of the Pareto front are spread in a uniform manner. While MID is one of the all-purpose metrics to evaluate convergence of the Pareto-based multi-objective optimization algorithm (Rashidnejad et al., 2018). The algorithm with a smaller value of MID has better performance in convergence. In addition, there is no doubt that a larger value of QM implies a more favorable algorithm due to the greater number of decision-making alternatives available to the decision makers. As shown in Table 4, the IMPSO algorithm has smaller values of SM and MID and has a larger value of QM. It can be concluded that compared to the NSGA-II algorithm, the IMPSO algorithm generates more efficient non-dominated solutions. Although the better performance of the IMPSO algorithm is at the expense of more

computation time, the increase in computation time is modest and acceptable given the enhanced performance.

Table 4
Experimental results of ten runs for IMOPSO and NSGA-II algorithms.

No	IMPSO				NSGA-II			
	SM	MID	QM	CPU(s)	SM	MID	QM	CPU(s)
1	0.168	0.750	32	70.80	0.185	0.912	22	64.06
2	0.146	1.122	31	70.50	0.112	1.953	20	63.08
3	0.294	1.111	29	73.00	0.161	1.519	21	64.17
4	0.117	1.494	28	70.57	0.436	2.885	23	61.67
5	0.220	1.146	29	73.40	0.424	2.054	19	66.83
6	0.107	0.975	30	72.96	0.354	1.512	23	61.40
7	0.239	0.753	33	71.38	0.642	1.073	19	62.13
8	0.231	1.065	30	73.65	0.148	0.726	22	63.37
9	0.271	1.493	28	70.65	0.103	1.249	24	63.04
10	0.368	1.478	28	72.56	0.114	1.788	21	62.58
Avg	0.216	1.139	29.8	71.95	0.268	1.567	21.4	63.23

6.2.2 Convergence

The Convergence process after several runs is critical for investigating the performance of the algorithms. The convergence of the algorithms is reflected by the minimum Euclidean distance after standardization between the non-dominated solutions in each iteration and the origin (Rashidnejad et al., 2018). Since the optimization problem in this paper is a minimization problem with two objectives, the non-dominated solution closer to the origin has a better performance. Fig. 7 illustrates how the solution approaches come to a stable state for the problem after the limited iterations. The convergence curves in Fig. 7 show that the distance from the origin decreases rapidly over the first 25 iterations for both the algorithms. It is worth noting that the IMPSO algorithm has a lower value than the NSGA-II algorithm from the earliest stage to the final stage. It indicates that the IMPSO algorithm is better at solving this problem. What's more, the curve of the IMPSO algorithm shows that it can keep making improvements until the later stage. It proves that the introduction of the niche sharing mechanism is indeed beneficial for the solution procedure to enhance the search capability and help the algorithm effectively avoid the local optimal trap.

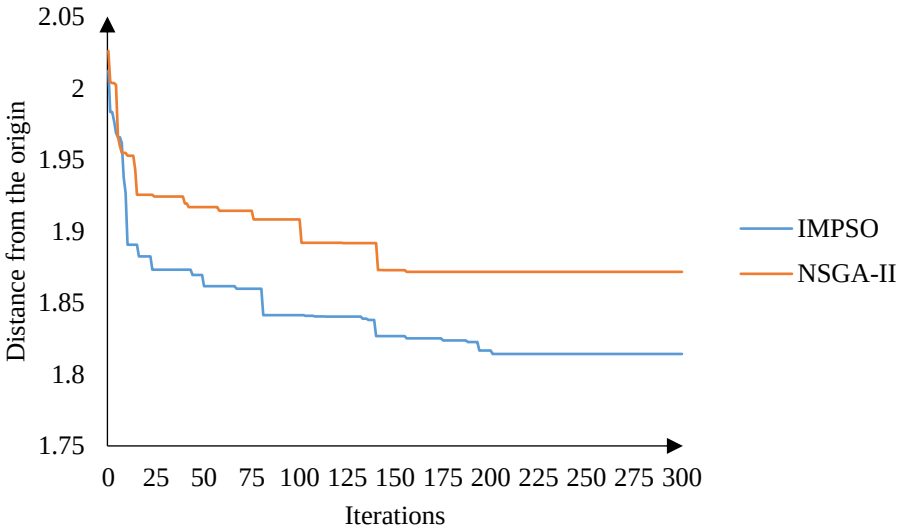

Fig. 7. The convergence process of the algorithms

6.3 Computation results

Similar to most multi-objective optimizations, the Pareto solutions obtained by IMPSO cannot directly provide decision makers with a specific scheduling scheme. Based on these Pareto solutions, we adopt the cost performance method to determine the ideal scheduling scheme. First, according to the procedure of the cost performance method proposed in Section 5.4, we can obtain the corresponding mean variability k_l ($l \in \{1,2\}$), sensitivity ratio δ_l ($l \in \{1,2\}$) and standardized sensitivity ratio ε_l ($l \in \{1,2\}$), the details of which are stated in Table 4. Fig. 7 illustrates the distribution of the sensitivity ratio after standardization.

Table 4
Corresponding parameters of the cost performance method.

No.	k_1	k_2	$\delta_1(\times 10^{-4})$	$\delta_2(\times 10^{-7})$	ε_1	ε_2
1	**0.879**	**1.138**	**0.080**	**7.886**	**0.000**	**0.267**
2	**3.392**	**0.654**	**0.310**	**4.528**	**0.001**	**0.153**
3	14.020	0.107	1.286	0.741	0.005	0.025
4	16.795	0.066	1.544	0.456	0.006	0.015
5	**6.807**	**0.275**	**0.628**	**1.891**	**0.003**	**0.064**
6	**4.205**	**0.312**	**0.389**	**2.140**	**0.002**	**0.072**
7	11.870	0.109	1.099	0.744	0.005	0.025
8	11.978	0.106	1.112	0.723	0.005	0.024
9	11.105	0.109	1.034	0.744	0.004	0.025
10	14.073	0.072	1.313	0.491	0.005	0.017
11	15.121	0.068	1.413	0.465	0.006	0.016
12	23.655	0.045	2.218	0.304	0.009	0.010
13	30.758	0.033	2.889	0.220	0.012	0.007
14	40.586	0.026	3.820	0.173	0.016	0.006
15	327.478	0.011	30.845	0.074	0.128	0.002
16	313.228	0.025	29.507	0.167	0.122	0.006
17	18.460	0.055	1.741	0.365	0.007	0.012
18	13.642	0.076	1.291	0.504	0.005	0.017
19	30.521	0.055	2.894	0.367	0.012	0.012
20	**26.199**	**0.223**	**2.486**	**1.468**	**0.010**	**0.050**
21	**22.206**	**0.225**	**2.111**	**1.480**	**0.009**	**0.049**
22	58.047	0.019	5.522	0.122	0.023	0.004
23	49.832	0.026	4.743	0.172	0.020	0.006
24	20.291	0.053	1.936	0.345	0.008	0.012
25	12.829	0.080	1.226	0.522	0.005	0.018
26	23.417	0.061	2.238	0.394	0.009	0.013
27	35.499	0.028	3.399	0.183	0.014	0.006
28	47.659	0.023	4.572	0.146	0.019	0.005
29	**570.214**	**0.009**	**54.735**	**0.056**	**0.226**	**0.002**
30	**543.890**	**0.065**	**52.211**	**0.414**	**0.216**	**0.014**
31	**38.229**	**0.071**	**3.680**	**0.458**	**0.015**	**0.015**
32	42.138	0.039	4.059	0.251	0.017	0.009
33	44.742	0.039	4.318	0.247	0.018	0.008
34	56.272	0.020	5.434	0.125	0.022	0.004
35	38.676	0.026	3.742	0.164	0.015	0.006

The solutions in bold are Pareto non-dominated solutions based on the standardized sensitivity ratio.

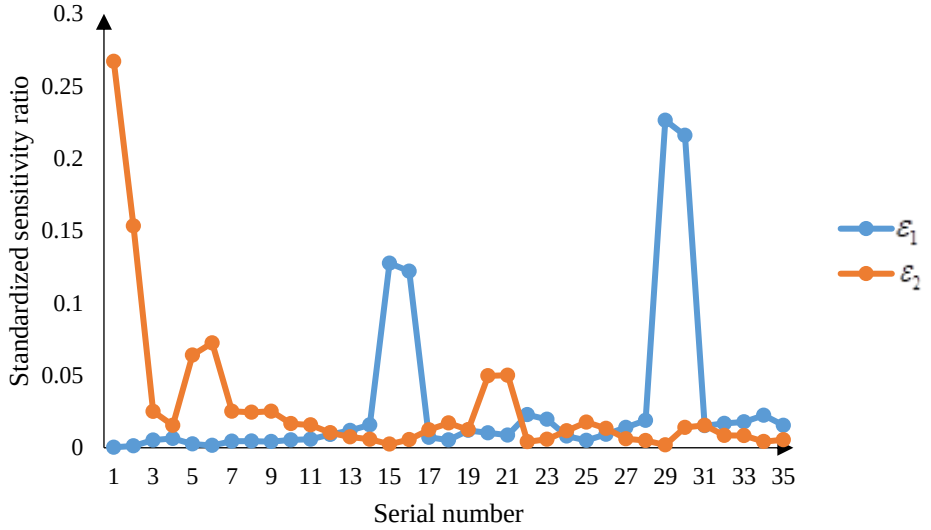

Fig. 7. Sensitivity ratio distribution after standardization.

According to Pareto dominance based on the standardized sensitivity ratio, 26 of the original 35 non-dominated solutions are eliminated. The remaining 9 solutions (i.e., the solutions in bold in Table 4) constitute a subset of Pareto non-dominated solutions, which further narrows the range of the ideal options for decision makers. In the Pareto subset, decision makers can effectively select an ideal option according to the Pareto frontier based on the standardized sensitivity ratio. In emergency management, for the sake of social responsibility, decision makers usually prefer the objective of responsiveness to that of cost. When the values of both the responsiveness objective and the cost objective are acceptable, the solution with the largest skewness to the responsiveness objective is better and is selected as the most suitable option. Therefore, the solution numbered 29 can be selected as the ideal solution, the skewness of which to the responsiveness objective has the highest value, which is 0.991. The corresponding scheduling scheme is shown in Table. 5. Under such a scheme, the value of the ecological environmental loss is 1.0418×10^{9} CNY, and the total cost is 1.553×10^{6} CNY.

Table 5
The ideal dynamic scheduling scheme.

No. of emergency fleets	Subordinate to	Route planning	Number of vessels	Quantity of oil booms (m)
1	Dalian	27-14-4-24-27	19	11,330
2	Yantai	26-9-2-13-7-26	26	15,130
3	Weihai	25-3-8-12-15-23-25	30	17,987
4	Dalian	25-1-6-5-10-21-16-25	36	21,377
5	Dalian	25-17-22-20-25	19	11,080
6	Yantai	26-19-11-18-26	19	11,102

6.3 Sensitivity analysis

In this section, we carry out a series of sensitivity analyses to show how changes in the parameters affect the computational results of the proposed model with time-varying factors. The parameters involved in the analysis include the shipping speed (vk), oil film drift speed (v_a, $a \in A$) and emergency time difference ($\hat{T}$). The selection of such parameters is because any change in the related factors can have a considerable impact on the values of the objective functions, and the values of these parameters exhibit a wide range of variation in the response to different oil spill accidents according to the interview survey results from the associated

maritime authorities.

6.3.1 Sensitivity to shipping speed

The impact of changing the shipping speed by -20%, -10%, +10% and +20% on the total loss of the ecological environment and the total response cost is illustrated in Fig. 8. Both objectives are sensitive to the changes in the shipping speed of the emergency fleets. However, the values of both objective functions are more sensitive to decreasing the shipping speed. This phenomenon is most likely due to the irregular pattern of oil film changes. In reality, the diffusion rate of the oil film area is not stable but rather increases with the expansion of the area. As the shipping speed decreases, emergency resources will take longer to reach the demand points, which allows the oil film to diffuse rapidly for a longer time, leading to a considerable increase in the demand for emergency resources. This increase in demand will result in a longer delivery time and higher consumption costs. When dealing with the oil film at the next demand point, such a phenomenon will be further intensified, similar to the bullwhip effect. Under the influence of a series of chain reactions, varying the shipping speed will lead to significant changes in both responsiveness and cost.

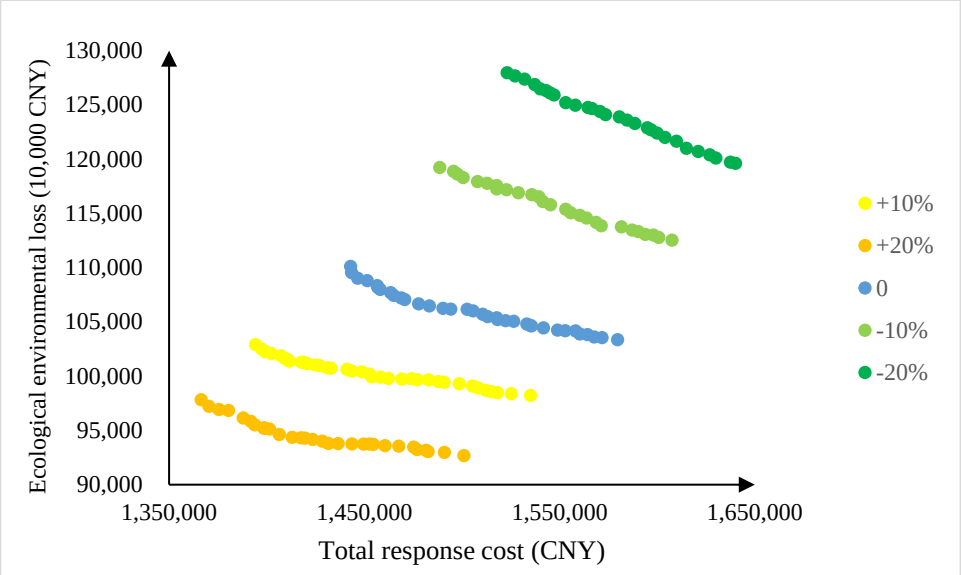

Fig. 8. Impact of varying the shipping speed.

6.3.2 Sensitivity to drift speed

The drift speed of oil films at sea is one of the main uncertain factors during the process of implementing emergency operations. Fig. 9 presents the sensitivity analysis outcome of the multi-objective model by investigating the impact of varying the drift speed by -20%, -10%, +10% and +20%. As shown in the figure, both the responsiveness and cost objectives vary with the drift velocity, but the trend is not obvious. Except for the increase in drift speed by 10%, none of the other scenarios have a positive impact on responsiveness. The -20% and +20% changes in drift speed not only fail to promote emergency efficiency but also expand the oil spill pollution area. Interestingly, reducing the oil film drift speed by 10% does not show any obvious effect on the emergency response, mainly because there is no direct connection between the drift velocity of oil films and responsiveness. When the oil film drifts toward the emergency fleet, the increase in drift speed can promote responsiveness, and vice versa. When the oil film drifts away from the emergency fleet, the increase in drift speed can reduce responsiveness, and vice versa. In actual emergency logistics situations, the sailing direction of the emergency fleet and drift direction of the oil spill are dynamic. Therefore, changes in the drift motion of the oil film will contribute to responsiveness only when it is in line with the transport activities of the emergency fleet.

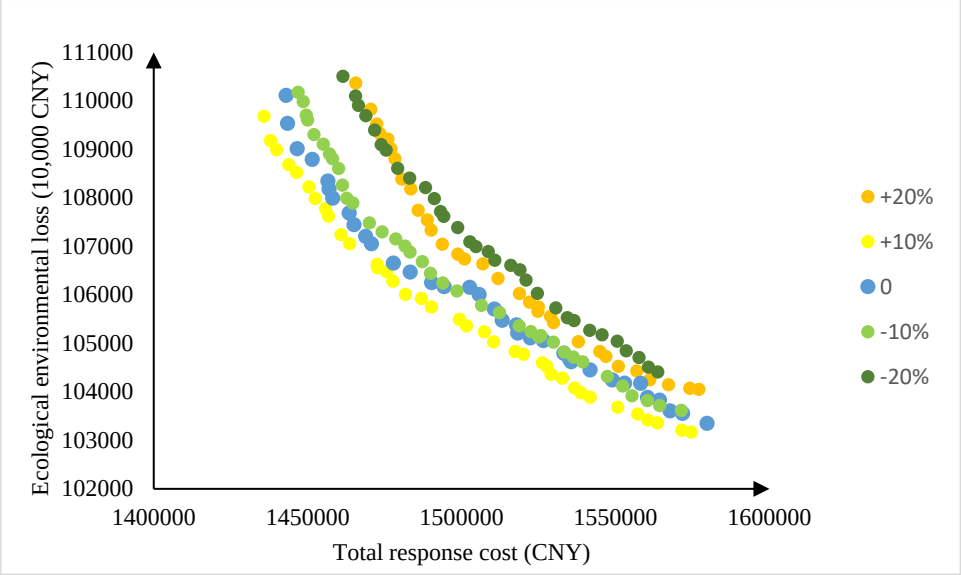

Fig. 9. Impact of varying the drift speed.

6.3.3 Sensitivity to differences in the emergency response time

When a major oil spill accident occurs at sea, the emergency response procedure will not be immediately activated. First, a monitoring method is used to detect the oil spillage and collect the relevant data, and then the decision-making organization will formulate the emergency scheme according to the actual situation. Hence, there is a time difference between the occurrence of the accident and the beginning of emergency operations. Fig. 10 represents the impacts of time difference changes of -20%, -10%, +10% and +20% on the objectives. The figure shows that the shorter the time difference, the closer the Pareto frontier is to the origin, which means that the more quickly emergency measures are taken, the more quickly the oil films can be controlled with less response cost. Nevertheless, both objectives are more sensitive to a decrease in the time difference. Similar to the effect of decreasing the shipping speed, the extension of the time difference also causes oil films to diffuse at a faster rate for a longer time, which will result in a larger contaminated area and the need for more emergency resources. Driven by this chain reaction, the longer the time difference, the more sensitive the values of the objective functions will be.

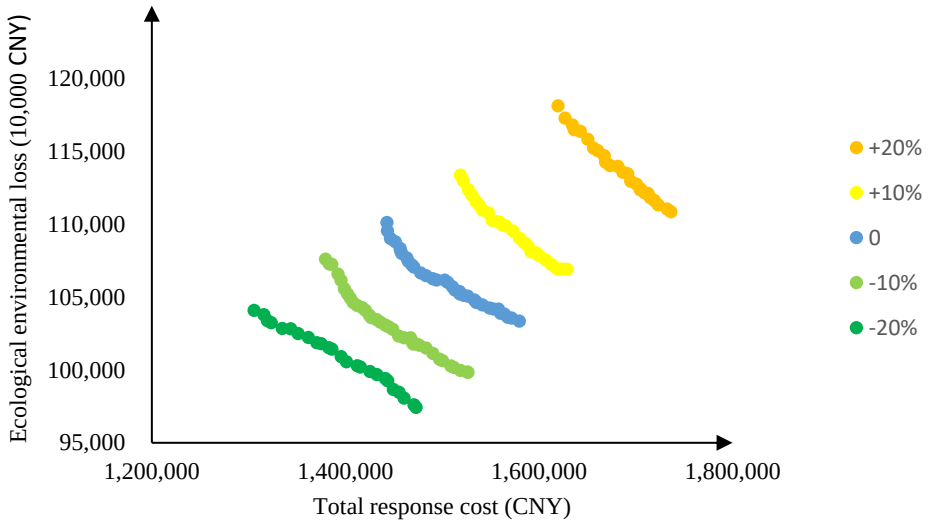

Fig. 10. Impact of varying the emergency response time.

6.4 Additional experiments

To make a comparison with the conventional methods (e.g., the time period planning horizon and the rolling planning horizon), we convert the dynamic model into a static counterpart based on the assumptions proposed in these methods that the demand in emergency resources of the demand points and the state of the associated transportation networks in emergency logistics remain stable over different time periods, and a single time period is usually as long as several days or a week (Lu et al., 2016; Maharjan et al., 2020). Since an oil spill response effort is not as long-lasting as a land-based disaster response effort (e.g., earthquake and hurricane), we simply consider the duration of the emergency response as a single time period. Herein, we modify the original multi-objective model with time-varying parameters as follows: 1) the oil film area does not change with time during the emergency response effort; 2) the oil film remains in its original position at all times; and 3) the responsiveness objective is changed to minimize the sum of the time necessary to complete the delivery of oil booms to all the demand points, while the cost objective remains the same.

To find the approximate solutions of the problem, ten runs are performed for the additional experiments with IMPSO, and the obtained Pareto frontier is shown in Fig. 11. Simultaneously, we use the cost performance method again to select the ideal solution in such a case. The corresponding parameters for the cost performance method are illustrated in Table 6. When we select the ideal solution according to the criterion of maximum skewness to the responsiveness objective, the solution numbered 23 can be selected, the skewness of which to the responsiveness objective is up to 0.864. Table 7 summarizes the specific scheduling scheme generated through the contrast model, of which the total time is 145.35 hours and the total cost is 8.71×10^{5} CNY.

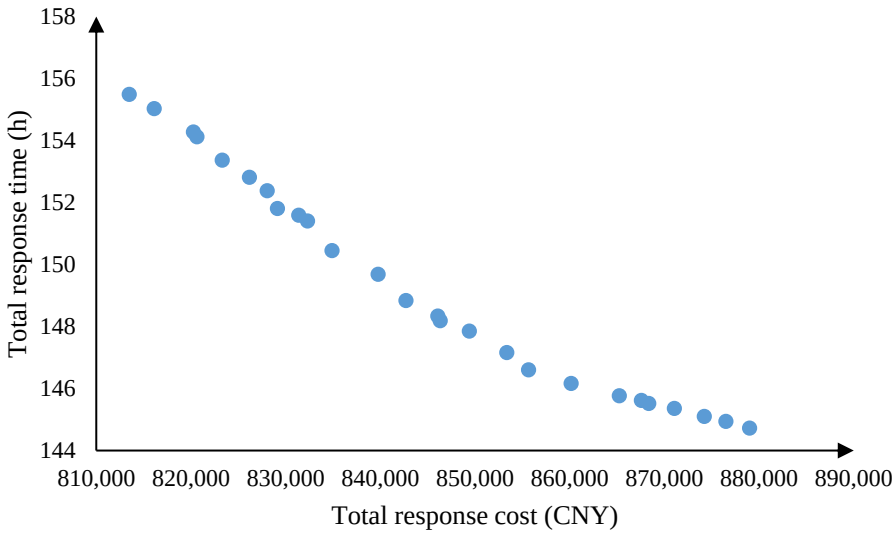

Fig. 11. Pareto frontier of the contrast model.

Table 6
Corresponding parameters of the cost performance method of the contrast model.

No.	$k_1(\times10^{3})$	$k_2(\times10^{-4})$	δ_1	$\delta_2(\times10^{-10})$	ε_1	ε_2
1	5.761	1.736	37.051	2.134	0.028	0.034
2	5.625	1.779	36.283	2.180	0.028	0.035
3	3.939	3.004	25.533	3.662	0.019	0.059
4	2.964	3.506	19.232	4.272	0.015	0.069
5	4.383	2.369	28.580	2.878	0.022	0.047
6	4.753	2.125	31.101	2.572	0.024	0.042
7	**3.090**	**3.797**	**20.282**	**4.585**	**0.015**	**0.074**
8	**6.150**	**3.109**	**40.513**	**3.749**	**0.031**	**0.061**
9	**7.678**	**1.489**	**50.651**	**1.791**	**0.039**	**0.029**

10	3.831	2.858	25.304	3.434	0.019	0.056
11	4.547	2.632	30.223	3.152	0.023	0.051
12	4.924	2.228	32.898	2.653	0.025	0.043
13	5.092	2.189	34.211	2.598	0.026	0.042
14	**4.211**	**3.689**	**28.391**	**4.360**	**0.022**	**0.070**
15	**5.449**	**3.489**	**36.769**	**4.122**	**0.028**	**0.067**
16	7.455	1.419	50.422	1.671	0.038	0.027
17	4.909	2.093	33.360	2.452	0.025	0.040
18	**7.168**	**1.706**	**48.893**	**1.994**	**0.037**	**0.032**
19	11.489	0.881	78.604	1.024	0.060	0.017
20	**14.383**	**0.704**	**98.674**	**0.814**	**0.075**	**0.013**
21	**11.830**	**0.966**	**81.243**	**1.114**	**0.062**	**0.019**
22	**12.247**	**0.951**	**84.165**	**1.095**	**0.064**	**0.018**
23	**14.550**	**0.705**	**100.101**	**0.809**	**0.076**	**0.012**
24	**13.331**	**0.755**	**91.880**	**0.864**	**0.070**	**0.014**
25	12.982	0.780	89.571	0.890	0.068	0.014
26	11.552	0.866	79.824	0.985	0.061	0.016

The solutions in bold are Pareto non-dominated solutions based on the standardized sensitivity ratio.

Table 7
The ideal scheduling scheme of the contrast model.

No. of emergency fleets	Subordinate to	Route planning	Number of vessels	Quantity of oil booms (m)
1	Yantai	26-16-8-18-26	12	7,129
2	Yantai	26-7-12-20-2-26	17	9,779
3	Dalian	25-3-4-15-21-19-25	20	11,897
4	Dalian	25-17-5-6-11-14-25	21	12,235
5	Yantai	26-9-22-24-23-26	16	9,453
6	Dalian	25-1-13-10-25	12	7,005

The comparison of the two schemes reveals that the quantity of oil booms in need and the total number of emergency vessels assigned in the time-varying model are significantly higher than those in the contrast model. When considering the diffusion motion of oil films at sea, as the oil film area gradually expands with time, the demand for oil booms at each demand point also gradually increases, as does the transportation capacity. Especially when there is a chain reaction caused by the interrelationship between the emergency response effort and the evolution of the oil spill, the growth of emergency resources and transportation capacity is much more significant.

In addition, there is also an obvious difference in the selection of ERRBs participating in the emergency response effort for the two schemes. Since the initial position of the contaminated area is close to the ERRBs of Dalian and Yantai and the quantity of demand for emergency resources is relatively small, in the contrast model only the emergency vessels from these two ERRBs participate in the emergency response. Nevertheless, in the scheduling scheme developed in the newly proposed model, ERRB Weihai also undertakes a considerable emergency task, which is due to two reasons. First, the demand for oil booms increases significantly when considering the diffusion motion of oil films. If we do not make use of the emergency resources reserved in ERRB Weihai and only rely on the other two ERRBs for the response, the cost will soar due to the excessive use of supplementary resources and vessels. Moreover, after a certain period of drifting, the oil films initially near the ERRBs of Dalian or Yantai will be closer to ERRB Weihai, so it is more efficient to assign emergency vessels from ERRB Weihai to transport and deliver oil booms to those demand points. From the specific scheduling scheme (presented in Table 5), we can learn that the demand points in the charge of

ERRB Weihai are all drifting to it, consequently supporting the above inference.

Through the above comparative analysis, it is obvious that the time-varying model can better reflect the reality and provide a more efficient decision to tackle an oil spill emergency. The contrast model leads to error-prone decisions. The associated emergency resource scheduling scheme obtained from the time-varying model is also highly compatible with the optimization objectives of both responsiveness and cost, meaning that it can tackle the oil spills with higher efficiency and lower cost.

7 Conclusions

In this study, we propose a dynamic multi-objective location-routing model with time-varying factors to better fit the requirements of a real-world emergency response to an oil spill accident. In view of the characteristics of the model, we develop the IMPSO algorithm to solve the problem. The Pareto solutions cannot directly provide decision makers with a specific scheduling scheme. To facilitate the decision making based on preference, we adopt the cost performance method to determine the ideal scheduling scheme. A numerical analysis with a real-large-scale oil spill accident in the Bohai Bay is conducted to illustrate the feasibility of the proposed approaches in practice. By comparing the performance metrics and convergence curves of the IMPSO and NSGA-II algorithms, it is demonstrated that the IMPSO algorithm outperforms the NSGA-II algorithm and is able to generate more efficient non-dominated solutions. In addition, we make use of a series of randomly generated numerical scenarios to check the sensitivity of the objectives to some critical parameters. The results of the sensitivity analysis show that the objectives of both responsiveness and cost are sensitive to these parameters, but the sensitivity of these objectives varies greatly depending on the influence of time-varying factors. To further evaluate the performance of the dynamic model with time-varying features, we conduct an additional experiment with a contrast model which removes all the time-varying parameters. After comparing the ideal schemes of the two models, a significant difference is found. Through the comparison analysis, the scheduling scheme based on the dynamic motion of the oil films is demonstrated to be more consistent with the actual emergency response situation for major oil spill accidents. The series of quantitative analyses will be helpful for investigating the proposed model and approaches to other multi-objective combinatorial optimization problems with time-varying factors.

Although our study fulfils several notable gaps between the literature and real demands on emergency logistics in oil spill accidents at sea, there are still a few limitations to be addressed in the future. First, we only propose a mono-resource optimization model for the response to oil spills. Actually, due to the vastness of the polluted area, the oil film conditions at diverse demand points could be different, which may require different cleaning steps with different emergency resources. The question regarding how to coordinate the scheduling of different emergency resources remains to be solved. Second, our work only takes into consideration the real scenarios in which the demand in emergency resources is comparable to the vessels' transportation capacity; in this case, the demand point can be met by one-time delivery. When the demand for resources at the demand points is greater than the vessels' capacity (e.g., oil dispersant and floating oil bladders), spilt multiple deliveries should be committed for transportation. In addition, compatibility issues exist between different resources and means of transportation; that is, different modes of transportation are applicable to different resources. Future work can be conducted by coordinating the transportation of emergency resources by different delivery and transportation modes (e.g., sea and air).

Acknowledgements

We would like to thank the anonymous reviewers and the editorial office for their thorough and constructive comments. They have helped to improve the quality of our work significantly. This research is supported by the National Natural Science Foundation of China (71974023, 71831002), the Fundamental Research Funds for the Central Universities (313209302, 3132019501) and the National Social Science Fund of China (18VHQ005). We also acknowledge the funding of the EU ERC 2019 Consolidator Grant under grant agreement No 864724 (TURST).

References

Abdolhamid, Z., Mehrdad, K., Ali, H.K., 2020. Multi-objective decision-making model for distribution planning of goods and routing of vehicles in emergency multi-objective decision-making model for distribution planning of goods and routing of vehicles in emergency. International Journal of Disaster Risk Reduction. 48, 101587.

Ahmadi M., Seifi A., Tootooni B., 2015. A humanitarian logistics model for disaster relief operation considering network failure and standard relief time: A case study on San Francisco district. Transp. Res. Part E: Logist. Transp. rev. 75, 145-163.

Ai, Y.F., Lu, J., Zhang, L.L., 2015. The optimization model for the location of maritime emergency supplies reserve bases and the configuration of salvage vessels. Transp. Res. Part E: Logist. Transp. Rev, 83, 170-188.

Alem, D., Clark, A., Moreno, A., 2016. Stochastic network models for logistics planning in disaster relief. Eur. J. Oper. Res. 255(1), 187-206.

Ando, A.W., Khanna, M., Amy, wildermuth, et al., 2004. Natural resource damage assessment: methods and cases. Illinois: Illinois waste management and research center, 25.

Baharmand H., Comes T., Lauras M ., 2019. Bi-objective multi-layer location–allocation model for the immediate aftermath of sudden-onset disasters. Transp. Res. Part E: Logist. Transp. rev. 127(1), 86-110.

Barron, M.G., 2012. Ecological impacts of the Deepwater Horizon oil spill: implications

for immunotoxicity. Toxicol. Pathol. 40, 315–320.

Berman, O., Larson, R.C., 2001. Deliveries in an Inventory/Routing Problem Using Stochastic Dynamic Programming. Transportation Science, 35(2):192-213.

Cao, C.J., Li, C.D., Yang, Q., Liu, Y., Qu, T., 2018. A novel multi-objective programming model of relief distribution for sustainable disaster supply chain in large-scale natural disasters. J. Cleaner Prod. 174, 1422-1435.

Charles, A., Lauras, M., Van Wassenhove, L.N., Dupont, L., 2016. Designing an efficient humanitarian supply network. J. Oper. Manage. 47, 58–70.

Comes, T., Wijngaards, N., Van de Walle, B., 2015. Exploring the future: runtime scenario selection for complex and time-bound decisions. Technol. Forecast. Soc. Chang. 97, 29–46.

Daly, K.L., Passow, U., Chanton, J., Hollander, D., 2016. Assessing the impacts of oil-associated marine snow formation and sedimentation during and after the Deepwater Horizon oil spill. Anthropocene 13, 18–33.

Daniel, R.R., Gina, G., Ruben, Y.P., 2020 Planning the delivery of relief supplies upon the occurrence of a natural disaster while considering the assembly process of the relief kits. Socio-Economic Planning Sciences. 69, 100682.

Eberhart, R., Shi, Y., 2001. Tracking and optimizing dynamic systems with particle swarms, Proceedings of the 2001 Congress on Evolutionary Computation, 1, 94–100, http://dx.doi.org/10.1109/CEC.2001.934376.

Fay, J.A., 1979. Physics Processes in the Spread of Oil on a Water Surface. Proceedings of the Joint Conference on Prevention and Control of Oil Spills, 463-467.

Faass J., 2010. Florida's approach to natural resource damage assessment: a short, sweet model for states seeking compensation. Ecological Restoration, 3, 28-39.

Ghasemi, P., Khalili-Damghani, P., Hafezalkotob, A., et al., 2019. Uncertain multi-objective multi-commodity multi-period multi-vehicle location-allocation model for earthquake evacuation planning. Applied Mathematics and Computation, 350, 105-132.

Gökalp, E., Ümit, B., 2020. A robust disaster preparedness model for effective and fair disaster response. European Journal of Operational Research. 280 (2), 479-494.

Hao, G.Z., Huang, L.W., Zhang, K., et al. 2020. Dual-objective emergency material dispatching in marine oil spill accident. Journal of Safety and Environment. doi: 10.13637/j.issn.1009-

6094.2019.1604.

Hoyos, M.C., Morales, R.S., Akhavan-Tabatabaei, R., 2015. Or models with stochastic components in disaster operations management: a literature survey. Comput. Ind. Eng. 82, 183–197.

Hu, C., Liu, X., Hua, Y., 2016. A bi-objective robust model for emergency resource allocation under uncertainty. Int. J. Prod. Res, 54, 7421–7438.

Huang, K., Jiang, Y., Yuan, Y., Zhao, L., 2015. Modeling multiple humanitarian objectives in emergency response to large-scale disasters. Transp. Res. Part E: Logist. Transp. Rev. 75, 1–17.

Huang, X.L., Ren, Y.T., Zhang, J.A., et al., 2020. Dynamic Scheduling Optimization of Marine Oil Spill Emergency Resource. Journal of Coastal Research. 107, 437-442.

Jebari, K., Bouroumi, A., Ettouhami, A.,. 2013. Fertilization Operator for Multi-Modal Dynamic Optimization. Lecture Notes in Electrical Engineering, 229, 475-489.

Kennedy, J., Eberhart, R., 1995. Particle swarm optimization. Proceedings of the Fourth IEEE International Conference on Neural Networks, 1942-1948.

Kunz, N., Van Wassenhove, L.N., Besiou, M., Hambye, C., Kovács, G., 2017. Relevance of humanitarian logistics research: best practices and way forward. Int. J. Oper. Prod. Manage, 37(11), 1585-1599.

Liu, J., Guo, L., Jiang, J.P., et al., 2018, Emergency material allocation with time-varying supply-demand based on dynamic optimization method for river chemical spills. Environment Science and Pollution Research. 25,17343-17353.

Liu, S.K., Leendertse J.J., 1981. A 3-D oil spill model with and without ice cover. Proceedings of the International Symposium on Mechanics of Oil Slicks. Proceedings of the International Symposium on Mechanics of Oil Slicks． Paris， France: Rand Corp.

Loree, N., Aros-Vera, F., 2018. Points of distribution location and inventory management model for post-disaster humanitarian logistics. Transp. Res. Part E: Logist. Transp. Rev. 116, 1–24.

Lu, C.C., Ying, et al., 2016. Real-time relief distribution in the aftermath of disasters – A rolling horizon approach. Transportation Res. Part E Logistics Transportation Rev. 93, 1–20.

Maharjan, R., Hanaokab, S., 2020 A credibility-based multi-objective temporary logistics hub location-allocation model for relief supply and distribution under uncertainty. Socio-Economic Planning Sciences, 70, 100727.

Moreno, A., Alem, D., Ferreira, D., et al., 2018. An effective two-stage stochastic multi-trip location-transportation model with social concerns in relief supply chains. European Journal of Operational Research, 269, 1050-1071.

Najafi, M., Eshghi, K., Dullaert, W., 2013. A multi-objective robust optimization model for logistics planning in the earthquake response phase. Transport. Res. Part E: Logist. Transport. Rev. 49, 217–249.

Oscar, R.E., Pavel, A., Christopher, B., 2018. Dynamic formulation for humanitarian response operations incorporating multiple organisations. International Journal of Production Economics. 204, 83-98.

Payam A.H., Mohammad R., 2019. Response planning for accidental oil spills in Persian Gulf: A decision support system (DSS) based on consequence modeling. Marine Pollution Bulletin, 140:116-128.

Ransikarbum K., Mason S.J., 2016. Multiple-objective analysis of integrated relief supply and network restoration in humanitarian logistics operations. International Journal of Production Research, 54 (1), 49-68.

Rashidnejad, M., Ebrahimnejad, S., Safari, J., 2018. A bi-objective model of preventive maintenance planning in distributed systems considering vehicle routing problem. Computers & Industrial Engineering, 120, 360-381.

Rezaei, M., Afsahi, M., Shafiee, M., et al., 2020. A bi-objective optimization framework for

designing an effcient fuel supply chain network in post-earthquakes. Computers & Industrial Engineering, 147, 106654.

Rezaei-Malek, M., Tavakkoli-Moghaddam, R., Cheikhrouhou, N., et al., 2016. An approximation approach to a trade-off among efficiency, efficacy, and balance for relief pre-positioning in disaster management. Transportation research part E: logistics & transportation review, 93: 485–509.

Sheu, J.B., 2007. Challenges of emergency logistics management. Transport. Res. Part E: Logist. Transport. Rev. 43(6):655-659

Sarhadi, H., Naoum-Sawaya, J., Verma, M., 2020. A robust optimization approach to locating and stockpiling marine oil-spill response facilities. Transport. Res. Part E: Logist. Transport. 141, 102005.

Sheu, J.B., 2010. Dynamic relief-demand management for emergency logistics operations under large-scale disasters. Transport. Res. Part E: Logist. Transport. Rev. 46, 1–17

Song, X.Y., Wang, J.G., Chang, C.G., 2017. Nonlinear continuous consumption emergency material dispatching problem. Journal of Systems Engineering 32 (02),163-176.

Tian, D.P., Shi, Z.Z., 2018. MPSO: Modified particle swarm optimization and its applications. Swarm and Evolutionary Computation, 41, 49-68.

Torabi, S.A., Shokr, I.,Tofighi, S., et al., 2018. Integrated relief pre-positioning and procurement planning in humanitarian supply chains. Transportation research part E: logistics & transportation review, 113, 123-146.

U.S. National Commission on the Deepwater Horizon Oil Spill and Offshore Drilling, Deep Water — The Gulf Oil Disaster and the Future of Offshore Drilling Report to the President. U.S. National Commission on the Deepwater Horizon Oil Spill and Offshore Drilling, USA, 2011, pp. 398.

Wang, H.J., Du, L.J., Ma S.H., 2014a. Multi-objective open location-routing model with split delivery for optimized relief distribution in post-earthquake. Transportation Research Part E Logistics & Transportation Review, 2014, 69, 160-179.

Wang, J., Wang, M.R., Wang, Y.Y., et al. 2014b. Collaboratively scheduling method of SAR resources for drifting objective in distress at sea based on greedy algorithm. Operations Research & Management Science 23 (2):116-123.

Wang, N., Wu, D., Huang, Q., et al., 2018. A quantitative method to select best option of Pareto non-dominated solutions: cost performance method. Systems Engineering —Theory & Practice 38 (3), 725-733.

Wei, X.W., Qiu, H.X., Wang, D.J., et al., 2020. An integrated location-routing problem with post-disaster relief distribution. Computers & Industrial Engineering, 106632. https://doi.org/10.1016/j.cie.2020.106632.

Xiong, W.T., Gelder von P.H.A.J.M., Yang, K.W., 2020. A decision support method for design and operationalization of search and rescue in maritime emergency. Ocean Engineering, 207, 107399.

Xu, S., Xu, Z., Liu, Y., 2016. Optimal dispatch of oil spill resources considering resource priority. IEEE International Conference on Intelligent Transportation Engineering. doi: 10.1109/ICITE.2016.7581311.

Yang, Z., Guo, L., Yang, Z., 2019. Emergency logistics for wildfire suppression based on forecasted disaster evolution. Annals of Operations Research. 283, 917-937.

Ye, X.D., Chen, B., Li, P., et al., 2019. A simulation-based multi-agent particle swarm optimization approach for supporting dynamic decision making in marine oil spill responses. Ocean and Coastal Management, 2019, 172, 128-136.

Yuan, Y ., Wang, D ., 2009. Path selection model and algorithm for emergency logistics management. Computers and Industrial Engineering, 56(3), 1081-1094.

Zajac, S., Huber, S., 2020. Objectives and methods in multi-objective routing problems: a survey and classification scheme. European Journal of Operational Research, https://doi.org/10.1016/j.ejor.2020.07.005.

Zhan, S., Liu, N., Ye, Y., 2014. Coordinating efficiency and equity in disaster relief logistics via information updates. Int. J. Syst. Sci. 45 (8), 1607–1621.

Zhang, J., Liu, H., Yu, G., et al. 2019. A three-stage and multi-objective stochastic programming model to improve the sustainable rescue ability by considering secondary disasters in emergency logistics. Computers & Industrial Engineering 135, 1145-1154.

Zhang, R., Chang, P.C., Song, S., Wu, C., 2017a. Local search enhanced multi-objective PSO algorithm for scheduling textile production processes with environmental considerations. Appl. Soft Comput. J. 61, 447e467.

Zhang, W.F., Yan, X.P., Yang, J.Q., et al., 2017b. Optimized maritime emergency resource allocation under dynamic demand. Plos One, 2017, 12(12):e0189411.

Zhang, Y.L., Chu, S.X., Fu, G., 1991. Study on mathematical model of oil spill pollution and its application. Research of Environment Science 4 (3), 7-28.

Zheng, Y.J., Ling, H.F., 2013. Emergency transportation planning in disaster relief supply chain management: a cooperative fuzzy optimization approach. Soft Computing, 17 (7), 1301-1314.

Zheng, Y.J., Chen, S.Y., Ling, H.F., 2015. Evolutionary optimization for disaster relief operations: A survey. Applied Soft Computing, 27, 553-566.